Liquid Flowmeter Using Thermal Measurement; Design and Application

Woojae Chung
Marquette University

LIQUID FLOWMETER USING THERMAL MEASUREMENT; DESIGN AND APPLICATION

by

Woo Jae Chung, B.S.

A Thesis submitted to the Faculty of the Graduate School,
Marquette University,
in Partial Fulfillment of the Requirements for
the Degree of Master of Science

Milwaukee, Wisconsin

May 2019

ABSTRACT

LIQUID FLOWMETER USING THERMAL MEASUREMENT;
DESIGN AND APPLICATION

WOO JAE CHUNG, B.S.

Marquette University, 2019

This thesis presents flowmeter devices which can measure flowrate, pressure and temperature of flowing liquid samples using thermal measurement method. Typical thermal mass flowmeter uses thermal properties of materials to obtain flow features only for gases. We designed and fabricated flowmeter devices with various functionalities such as: measuring properties of flowing liquid and identifying the type of liquid samples.

Thermal measurement methods using temperature sensor is a key of our flowmeter's working principle. The thermal mass flowmeter consists of a glass capillary, a tungsten wire heater, and a resistance temperature detector (RTD) sensor. The heater and sensors are integrated on the surface of the glass capillary. Noncontact flow measurement between sensor and liquid sample prevents flow disturbance and corrosion of sensors. When robustness and sensitivity are required for flow measurement, the thermal mass time of flight (ToF) measurement method, along with its simple readout, make it a great candidate for industrial and vehicle applications. The heat traveling time measurement is the method that measures the time of flight of thermal mass from heating site to sensing site. Depending on the flowrate of fluid and thermal diffusivity of the liquid sample, the heat traveling time differs.

However, low response speed and low sensitivity characteristics are drawbacks of thermal measurement methods, which are influenced by thermal properties of materials and structural design. To increase sensitivity of our flowmeter, we fabricated and designed the device using different component variables such as: size and thickness of RTD sensors, heating element, and glass tube thickness. Also, the flowmeter introduced in this work has two different types based on their size and they enable large flow range measurement. Micro-flowmeter can measure flowrate less than 100 μl/min and macro-flowmeter measures flowrate from 1 to 10 gallon per minute (GPM) of deionized (DI) water.

In this work, we used a number of techniques to increase the functionality of our device. Bypass system enables to measure high range of flowrate. Also, we designed gravity-driven flowrate calibration system to generate accurate flowrates. Moreover, we developed flowrate monitoring system to improve the performance of calibration system.

AKNOWLEDGMENT

Woo Jae Chung, B.S.

I would like to take this opportunity to thank my family. The completion of this thesis would not have been possible if not for the guidance and encouragement of my family. I want to thank my advisor, Dr. Chung Hoon Lee, Dr. James Richie, Dr. Simcha Singer for everything that they have taught me in past 2 years. I would specifically like to thank Prof. Chung Hoon Lee for the time and support he has invested in me to move forward and complete my thesis.

In addition, I want to thank all of the Nanoscale Devices Laboratory previous and current members, especially Rafee Mahbub for his help in the lab with fabrication and discussions regarding my work.

I dedicate this work to my parents and my sisters for the support they have provided me during my entire Master program, without their support this could be a lot harder to accomplish.

TABLE OF CONTENTS

LIST OF TALBES

LIST OF FIGURES

Chapter 1 Introduction

Measurement of the flow of a fluid is generally a critical parameter of many processes at either science or industry. In most operations, measuring flow of fluid, either gas or liquid, can be linked to the basic “recipe” of the process which is about knowing the right fluid at the right place and the right time. The flow variable affects many other process variables such as pressure, temperature, and chemical content. Flow measurement is essential to maintain proper system operation, and to assure the best relation between quality and cost of manufactured product. [1][2]

Equally, flow measurements must consider their ability to conduct accurate measurements which are tightly related to product quality and safety issues. Otherwise, the inaccurate measurement of flow, or the failure to take such measurements, can cause serious or even disastrous results. Considering that point of view, this thesis work investigates the thermal transfer phenomena at
flowing fluid condition and also provides new type of flowrate measurement method as a strong tool to develop the scope of flow measurement applications and processes. [1][2]

This chapter begins with an introduction to the basic history of flow measurement and brief concepts of different flowmeters and their technologies. Past and current flow measurement techniques are introduced with emphasis on the scope of the applications. As much as it is important for the new flowmeter technology to overcome the previous limit and develop its potential, our motivation and approach in the following section are focused on advantages of application with flowmeter device with new flow measurement system. Finally, overall structure of this thesis is presented in the last section of this chapter.

1.1 Flow measurement

In general, fluid flow measurement is investigating techniques for the features of fluids and flow velocity, volume, pressure and temperature using different methods. Since accurate background of flow measurement is needed to embark on developing a flow measurement system, definition of “Fluid flow measurement” is presented below.

Fluid - A substance that has no fixed shape and yields easily to external pressure; a gas or especially a liquid.

Flow - a. (of a liquid, gas, or electricity) move steadily and continuously in a current or stream.

b. Proceed or be produced continuously and effortlessly.

Measurement - a. The action of measuring something.

b. The size, length, or amount of something, as established by measuring.

Combining these three definitions into one definition for fluid flow measurement shows:

Fluid flow measurement - The action of measuring the amount of unfixed substance that moves steadily and continuously in a piping system. [3]

Flow measurement has developed over the years in different ways. The form of development varies in response to measurement under different types of fluids, flow rate ranges, and conditions of flow. [3]

Flow measurement started over 4000 years ago from Roman times. They measured water flow to control allocation from their aqueducts to each house. After that, flow measurement evolved for purpose of precision measurement based on solid science and technology.

One of the well-known examples is the development of head meter which was invented by Castelli and Tonicelli in the early 1600's. They determined that the rate of flow

was equal to the flow velocity times the area, and that discharge through an orifice varies with the square root of the head. We can show this with a simple equation (1) below:

$$Q = V \times A \quad (1)$$

where Q is the fluid flow through the pipe, V is average velocity of the flow, and A is the cross-sectional area of the pipe.

Many other works have been published since these initial works, making it possible to develop other areas of flow measurement and meters such as vortex shedding, ultrasonic, magnetic, turbine, and laser. These measurement technologies are introduced in the following section.

Even though there are many flowmeter systems, fluid flow is not always possible to measure accurately without having smooth and continuous stream. Some requisites and limitations are required for flowing fluid. Basically, fluids need to have a steady state mass flow, clean, homogenous, Newtonian and stable with a single-phase non-swirling profile with some limit of Reynolds number. In case these conditions are not met, then the measurement error can be raised and in some cases measurement cannot be attempted until the unexpected flows are rectified. [3]

1.2 Flowmeter technology

The importance of monitoring or controlling the flow of various fluids has been emphasized in both science and industry. Fluids flowing through pipes or ducts have a wide range from oils with high viscosity to light gases. It is not an easy engineering task to measure various types of fluids with single measuring principle. As a result, flow measurement has many different principles and techniques to satisfy each particular fluid type. At the same time, the flow measurement methods have continuously changed according to the needs of

industry, such as high accuracy and low manufacturing cost.

Flow meters may be classified by working principles into four groups: volumetric, mass, inferential and velocity flow meters. Volumetric and mass flow meters measure flow directly. On the other hand, inferential flow meters measure flow indirectly and they measure the flow from some physical phenomenon. Differential pressure, variable-area, and target flow meters are typical examples of inferential flow meters. [4][5]

Measuring flow directly is very common method in flow industrial field. There are two main methods, which are volumetric and mass flow measurement method. Users need to choose the method that is proper to use in their process. In this section, these two different flow measurement methods are summarized. [6]

First, volumetric flow measures the volume of fluid that passes a perpendicular section of a fluid tube per unit of time.

Equation for the volumetric flow of a liquid through a pipe can be simply expressed as:

$$Q_{Volumetric} = \iint_S \overrightarrow{v(x,y)}\,\vec{n}\,dx\,dy \quad (2)$$

where $\overrightarrow{v(x,y)}$ is the fluid's velocity, and $\vec{n}$ is the unit-vector normal to the perpendicular section; dx and dy are the infinitesimal elements of cross section area of the tube in direction of x and y.

In this equation, compressibility and sensitivity to temperature and pressure variations are neglected as we consider that the flow is in fully developed and steady state condition. Figure 1-1 shows the overall element of volumetric flow measurement from the above equation.

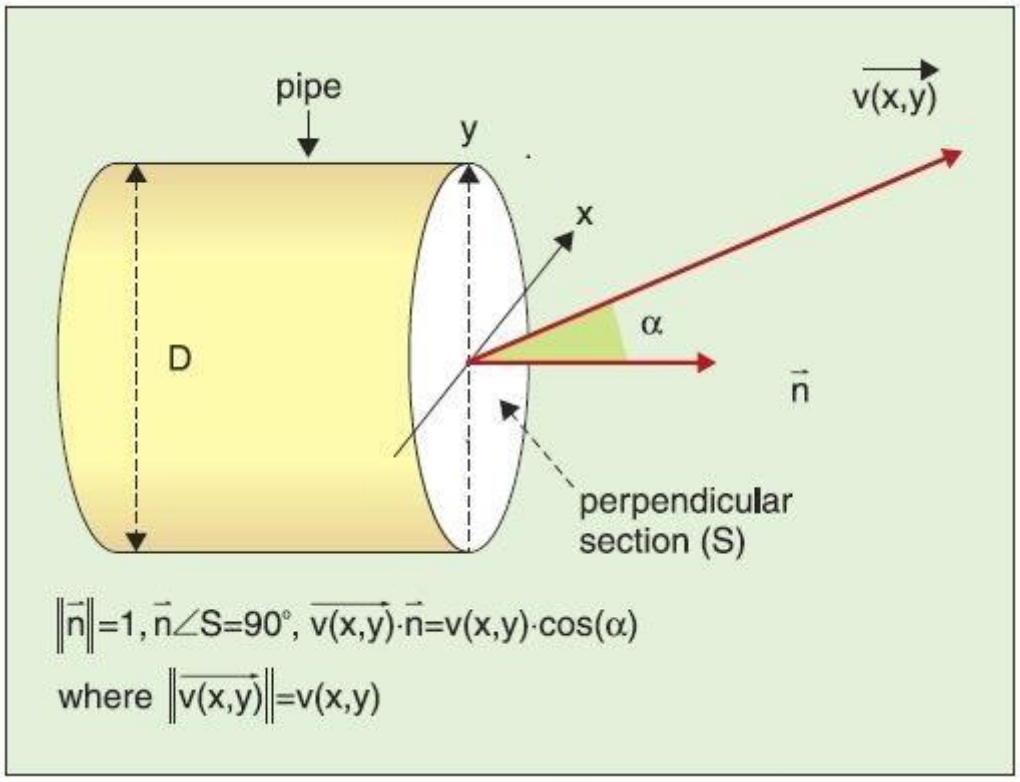

Figure 1-1. A pipe diagram labeled with the geometric parameters used to evaluate the volumetric flow

In contrast, mass flow meters describe the mass of the fluid passing the perpendicular section of a fluid pipe per unit of time. When temperature, pressure, and density of fluid are constant, the mass flow is given by:

$$Q_{Mass} = \iint_S \rho \cdot \overrightarrow{v(x,y)} \cdot \vec{n}\, dx\, dy \quad (3)$$

$$\rho = \frac{\mathrm{M}}{\mathrm{V}} \quad (4)$$

where $\overrightarrow{v(x,y)}$ and $\vec{n}$ represent the fluid's velocity and unit vector respectively (same as volumetric flow equation). The fluid's density is ρ. It is the mass per volume unit where M is mass and V is volume. [6]

Unlike volumetric and mass flow meters, inferential flow meters measure flow indirectly which means that they do not use mass and volume as measurement source.

Inferential flow meters use other measurable properties which are associated with fluid flow such as temperature or pressure. They have been used in many industrial applications due to their advantages, such as low cost and robustness. However, inferential flow meters may not have sufficient accuracy, certainty and linearity for some applications. [7][8]

One inferential flow meter is the differential pressure flow meter. Measuring a differential pressure between two pressure points is the operating principle of differential pressure flow meters. By inserting flow restriction at fluid guide, pressure must increase or decrease by the point due to the mass conservation principle. Orifice, nozzle, and Venturi types are the most common differential pressure flow meters used in industry. [7][9]

Another inferential flow meter is thermal mass measurement flow meter. Thermal flow meters utilize the thermal properties of the fluid to measure the flow rate. In a typical thermal mass flow meter as shown in Figure 1-2, there is a heater and temperature sensor close to each other in the pipe. A constant amount of heat is continuously applied to the heater and some of this heat is lost due to the flowing fluid. As the flow passes over the heat probe, it carries away heat. The heat loss depends on the mass flow rate, the heat capacity of the fluid, and the temperature difference between the probe and the fluid. Since the heat capacity of the fluid is known and the temperatures are monitored in real-time, the mass flow rate can be determined from the heat loss. Typically, flow can be identified by measuring amount of energy to maintain constant temperature of probe.

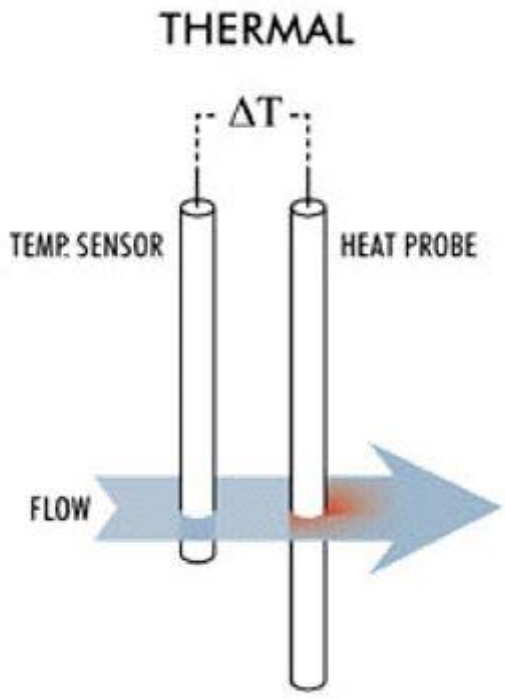

Figure 1-2. Principle of thermal mass flowmeter

There are many different types of flow meters which use different measurement methods that we introduced in this section. Each flow meter has advantages and disadvantages depending on applications. Table 1-1 summarizes the working principle, major application, advantages, disadvantages and variants of different flowmeter types.

Table 1. Flow Meters Types and their Main Characteristics

Flow Meter Type	Primary Working Principle	Quantity Measured	Advantages	Disadvantages	Meter Name
Differential pressure	Pressure drop caused by pipe's restriction	Volume (versatile – almost all gases and low viscosity liquids)	low-cost, versatile, robustness, variety of versions,	square root dependence, affected by pressure and density changes, high pressure drop (exception for nozzles)	Orifice, nozzle Venture, elbow, v-cone, Pitot tube, Annubar
Turbine	Rotating device	Volume (lubricating fluids)	no supply power requirements, extreme temperatures and pressures, certified for gases	only for low viscosity, moving parts, sensitive to contamination and vibration	single rotor, dual rotor, paddle wheel, propeller, tangential
Variable Area	dynamic balance (impulsion, weight and dragging)	Volume (liquid and gas applications with enough density)	Low-cost, no supply power requirements, simplicity, versatile	Vertical installation, constant pressure loss (inaccuracy low fluid's flow), affected by density and temperature changes	Rotameters different variants of float designs and sensing systems
Magnetic	Electromagnetic induction	Volume (almost all measurements as long as the conductivity is above a minimal value)	No moving parts, non-invasive, no pressure loss, no dependence of flow regime, not affected by temperature, density, conductivity and concentration changes	Only liquids applications, lower conductivity limit (0.05 μS/cm)	magnetic DC no electrodes two-wire partially full
Oscillatory	Coand effect	Volume (application to a large variety of liquids as long as RN is above a minimal value)	No moving parts, robustness, suitable for different fluid types (gas, liquid, steam), linear relation between measurement and fluid flow	Fluids that exceed a minimum velocity RN restriction, fluids with viscosity above a minimal value, complex signal's conditioning	Fluidic vortex
Target	Force of the fluid in a fixed body (target)	Volume (clean fluids, minimum movement quantity)	Low-cost, good performance in large pipes	Restrictions on RN, fluid's velocity, material of construction, low accuracy, almost impossible calibration	Target
Positive Displacement	Measurement of fixed fluid's volume per rotation	Volume (clean and non-abrasive liquids)	High accuracy, no supply power requirements, bidirectional operation, no RN restrictions	Only for liquids, high pressure drop, moving parts, sensitivity to contamination and overloading	helical gear, nutating disc, oscillating piston, oval gear, rotary
Ultrasonic	Acoustic waves or vibrations	Volume (clean liquids and some gases, but problematic for the last)	No moving parts, it could be non-invasive (transducers are outside the pipe), no pressure drop, linear relation between measurement and	Good accuracy only for liquids, error due to deposits, errors caused by gas bubbles, affected by sound, velocity,	Doppler transit time pulse repetition

			fluid's flow, on line calibration	temperature, concentration and density changes	
Insertion	Measurement of fluid's velocity in critical positions (e.g.: pipe's axis)	Volume (liquids, gas and steam in large pipes)	Depends on transducer types because it can be implemented using almost all flow meter's working principles	Only large pipes, requirement of data processing for acceptable values of accuracy, RN restriction (turbulent flow regime), large pressure drop	one for each type of transducer (metering principle)
Correlation	Correlation of measurement data captured in different positions	Volume (depend on flow meter type use for correlation purposes)	Typically non-invasive measurement method	(depend on flow meter type use for correlation purposes)	one for each type of transducer (metering principle)
Open Chanel	Sheet of fluid above a crested dam or variable height in a restriction(Parshall)	Volume (liquid flow measurements usually in irrigation, drains and water works systems)	Unique solution for measurements in open channels (e.g.: irrigation systems, river flows)	Pressure loss, not versatile	Weirs Parshall flume
Coriollis	Conservation of angular momentum	Mas (measurement of: liquids, gases with restrictions, harsh chemicals, density)	True mass measurement, no RN restrictions, high accuracy, unaffected by pressure, temperature and density	Acceptable accuracy only for liquids, vibration sensitivity, large size limitations	Coriollis Hydraulic Wheatstone bridge
Thermal	Thermal properties of materials	Mass (measurement of gases)	True mass measurement, robustness for industrial and vehicle applications, large flow range	Only for gases, non-linear inference measurement of mass, non-linear output signal, bubbles sensitivity	Hot Wire Anemometer

Table 1-1 Different types of flowmeter

1.3 Motivation of research

Flow measurement technology, as described in the previous section, offers many different types of sensors designed for measuring not only flow rate but also different properties of the fluid conditions such as pressure, temperature, and fluid types. While some sensors are specialized to use only one property of measurement with a specific requirement, a few others can use multiple items simultaneously with some requirement restrictions.

Among the flow measurement sensors, a thermal mass flow measurement device can measure flow and temperature simultaneously. It can also measure pressure in specific

configurations if certain conditions are met. A thermal device can simplify the measurement configuration of flow, pressure, and temperature measurements and become a powerful flowmeter due to simplification. Simplifying the sensor configuration would be essential not only in attaining low cost, but also in reliable operation.

However, the typical thermal mass flow measurement technology requires the thermal and material information of a liquid/gas prior to the measurement. In addition, there are some drawbacks of typical thermal mass flowmeter as we described in Table 1. We introduced more specific information about the comparison between typical thermal mass flow measurement device and thermal mass time of flight measurement method in chapter 2.

The goal of this thesis is to develop a flow measurement sensor and measure fluid properties by using the thermal mass Time of Flight (ToF) measurement method. In this work, we introduce a micro and macro machined thermal measurement device to measure liquid flow rates and temperature simultaneously. This ToF method provides high accuracy of flow measurement with fast response time at sensing element due to the size of the device by taking the advantage of the scaling law in micro-technology.

However, it is not easy to make flow measurements with high accuracy performance. Even when there is small noise, vibration, or dirt, measurement error can be affected by those factors. The typical accuracy of flow meters varies between 0.2\% and 5\% of its full-scale range (FSR). In the following section in this chapter, the strategies to approach the goal are discussed. [3]

1.4 Approach

In this work, we design and develop two main types of thermal flow meters with the capability to measure a wide range of flow rates. For applications that require the precise measurement of small flow rates, on the order of nl/min to μl/min, a micro-machined, MEMS-based flow meter has been developed. The flow meter consists of two thermal elements (a heater and a temperature sensor), a microfluidic channel, and electrical interfaces integrated on a silicon chip. A Resistive Temperature Detector (RTD) is used as the temperature sensor which has a resolution of 1mK. It can be used for determination of extremely low flow rate (nl/min). The RTD sensor is made of nickel metal, and it is deposited on top of the substrate using thermal evaporation.

The second type of flow meter has been developed to measure flow rates on the order of mL/min up to GPM (Gallon Per Minute). This device consists of a thin-wall glass tube, a heater, and integrated RTD sensors. For this project, we have different glass tube substrates distinguished by their wall thickness. The structural parameters of each substrate are presented in chapter 3. The thick-wall glass tube is more robust and easier to fabricate, while the thin-wall glass tube has higher sensitivity and is suitable for low electrical power applications.

For glass tube sensor, we can connect the sensor directly to the main flow pipe if the flow rate is not higher than 500 ml/min. For higher flow rates, we designed a bypass system which enables the measurement of flow rates up to 10 GPM. The bypass system has a fixed main pipe diameter with 8 different orifice sizes. By changing the orifices, we can shift the measurable flow rate ranges up or down.

We propose using the thermal time of flight (TOF) measurement method to determine the flow rate. As described in chapter 3, the thermal mass flow measurement requires the thermal properties of the liquid/gas. In the case of the TOF method, the heater generates a heat pulse or pulses and the temperature sensor detects the temperature change after a time delay.

Because the time delay of the temperature is measured, the thermal properties of the liquid/gas sample are not necessary to calculate the flow rate. By knowing the TOF in seconds and the diameter of the channel, we can determine the flow velocity. In our experiment, we use thin tungsten wire as the heater element. We utilize various amounts of current[A] for the amplitude of the heat pulse with different time durations. For the sensor, we evaporated 50 nm of nickel using a shadow masking technique on the outside of the glass tubes.

After optimization of our flowmeter device and sensors for precise measurement, we started the calibration process and repeatability test with sample devices. There are two test benches where we have tested our devices. The first test bench is water calibration system, which is capable of controlling the flow rate from 1GPM to 50GPM, invented by BadgerMeter, a flow measurement and control technology commercial company. The second calibration system is a gravity-driven flowrate system. This is made in our laboratory to measure low flowrates less than 10 ml/min range. Detailed specification and working principle of these two flowrate control systems are introduced in chapter 4.

1.5 Thesis outline

This thesis is divided into five chapters, where each chapter contains its own concept and, at the same time, all of the five chapters are intimately connected to one another. This thesis starts by introducing flow measurement and reviewing the past and current technologies of it with its challenges and limitations. In the second chapter, the operation principle of our flowmeter device is introduced, and the analysis and phenomena of the thermal system is presented. In the next chapter, two different scales of flowmeter, which are micro and macro size are designed and the fabrication of the devices are described. The measurement result and the data analysis and discussion are explicitly presented in the next chapter. Ongoing research and future works are reviewed in the final chapter. The brief summary and the organization of each of five chapters are presented in the next few pages.

In the first chapter, we define the terminology of the word 'Fluid flow measurement' to establish scientific background for this work and help both reader's and writer's understanding. Flow measurement technology and its applications are introduced along with highlighting the advantages and disadvantages of each flowmeter. The motivation of our work is presented based on the limitation and challenge of the current flowmeter applications. The strategy to approach our measurement objectives is presented in the last part of this first chapter.

Chapter 2 starts by describing heat transfer phenomena which is necessary to understand the main concept of our flow measurement method. Three different heat transfer phenomena: conduction, convection, and radiation are introduced in detail. Other analysis for thermal system is also covered in this chapter to support the measurement principle and techniques. In addition, the electrical analogy and its circuit model for analyzing heat transfer is presented.

Chapter 2 continues by introducing our new measurement method, thermal mass time of flight method. Principle of the method and overall measurement configuration is presented with the description of each device element. Explanation of heat pulse idea and two different pulse sources are introduced in this chapter as much as it is important for our thermal time of flight method. This chapter ends by presenting the flow visualization techniques, which helps to understand thermal transfer with expression of visual images.

In chapter 3, fundamental descriptions of our flowmeter design are provided by suggesting strategies for approaching the project goals. This chapter shows two different types of flowmeter, which are divided by size. At the beginning of this chapter, design of micro-fabricated flowmeter is presented with some required micro fabrication techniques. Device material and fabrication processes are also included in this chapter. The largest part of chapter 3 shows how the macro size thermal time of flight flowmeter is fabricated and designed. This chapter focuses on presenting the principles of the elements of the device. Pictures and a 3-D drawing of the actual device are included in the last part of this chapter to help understand the device configuration.

Chapter 4 contains the experimental measurement method and the results. The details of measurement setup including mechanical and electrical equipment opens this chapter. As our test bench, flowrate generation and control system are also described in detail. The experimental results are presented for each application in the discussion section.

The final chapter, chapter 5, provides a summary of current work. General conclusion of presented research is made at the first part of the chapter. In the second part, ongoing experimental support is briefly introduced. In continuation, the potential applications of the research are discussed by suggesting several future works with developed device.

Chapter 2 Device design and principle of operation

Fundamental understanding of the origin of heat and heat transfer phenomena is essential for designing devices where thermal measurement methods are used for detection and quantization. In addition, the overall thermal system of the measurement device needs to be well analyzed according to the principle and method.

This chapter concentrates on providing the scientific background of heat transfer phenomena in fluid flow devices. Thermal mass time of flight method is also introduced as a model for the technology of our flow meter device. In the last section of this chapter, there is a consideration for device design which is based on thermal properties and its heat transfer.

2.1 Heat transfer phenomena

Heat is the energy that transfers from one system to another as a result of temperature difference. Heat transfer is the phenomena that deals with the rates of such energy. The main subjects of heat transfer are determining the rates of heat transfer to or from a system, the times of heating or cooling at the period, and the variation of the temperature as well.

Heat transfer deals with systems that lack thermal equilibrium. The presence of a temperature difference is the basic requirement for heat transfer. There can be no net heat transfer between two systems that have the same temperature. For heat transfer, the driving force is the temperature difference, just as the voltage difference is the driving force for electric current flow and pressure difference is the driving force for fluid flow.

Two thermodynamic laws are essential to understand heat transfer and the laws become the framework for transfer phenomena. The first law shows that the rate of energy transfer into a body should be equal to the rate of increase of the energy of it. The second law requires that heat be transferred in the direction of decreasing temperature. It is the same as the electric

current flowing in the direction of decreasing voltage or the fluid flowing in the direction of decreasing total pressure.

In the following section, three different modes of heat transfer will be presented: conduction, convection, and radiation. All modes of heat transfer require the existence of a temperature difference, and all modes are from the high temperature medium to a lower temperature one. [10]

2.1.1 Conduction

Conduction is the energy transfer from the more active particles of an object to neighboring less active ones due to the interactions between the particles. Conduction can take place in solids, liquids, or gases. In case of gases and liquids, collisions of the molecules during motion and diffusion of them make conduction. In solids, conduction occurs by the vibrations of the molecules in a substance and the energy transport by free electrons. [10][11]

In this work, we deal with conductive heat transfer in solid due to the fact that conduction is dominant in solid mode. The rate of heat conduction through a medium can be explained by the geometry of the medium, its thickness, and the material of the medium, as well as the temperature difference across the medium.

The rate of heat conduction through a plane layer is proportional to the temperature difference across the layer and the heat transfer area, but is inversely proportional to the thickness of the layer. That is Fourier's law and it is the fundamental differential equation for heat transfer by conduction. The law is applicable at any location and at any time.

$$\text{Rate of heat conduction} \propto \frac{(Area)(Temperature\ difference)}{Thickness}$$

$$\dot{Q}_{cond} = kA\frac{T_1 - T_2}{\Delta x} = -kA\frac{\Delta T}{\Delta x}\ [W] \quad (5)$$

where the rate of heat conduction is $\dot{Q}_{cond}$, plane wall of thickness $\Delta x = L$ and area is A. $\Delta T = T_1 - T_2$ is the temperature difference across the wall and k is the thermal conductivity of the material.

In the limiting case of $\Delta x \to 0$, Fourier's law of heat conduction can be rewritten as:

$$dQ \propto A\left[\frac{-dT}{dx}\right] \quad (6)$$

$$dQ = kA\left[\frac{-dT}{dx}\right] \quad (7)$$

$$dQ = -kA\left[\frac{dT}{dx}\right] \quad (8)$$

Here dT/dx is the temperature gradient, which is the slope of the temperature curve on a T-x diagram, at location x. The negative sign in equation is due to the fact that with an increase in x, there is a decrease in T.

Furthermore, we can obtain a general relation for Fourier's law of heat conduction by considering thermal distribution in three-dimensions. In rectangular coordinates, the heat conduction vector can be expressed in terms of its components as:

$$\dot{Q} = \dot{Q}_x\vec{\imath} + \dot{Q}_y\vec{\jmath} + \dot{Q}_z\vec{k} \quad (9)$$

where $\vec{\imath}, \vec{\jmath},$ and $\vec{k}$ are the unit vectors, and $\dot{Q}_x, \dot{Q}_y$ and $\dot{Q}_z$ are the magnitudes of the heat transfer rates in the x-, y-, and z-directions, which again can be determined from Fourier's law as:

$$\dot{Q}_x = -kA_x\left[\frac{\partial T}{\partial x}\right], \dot{Q}_y = -kA_y\left[\frac{\partial T}{\partial y}\right], \quad \text{and } \dot{Q}_z = -kA_z\left[\frac{\partial T}{\partial z}\right] \quad (10)$$

As a result, heat transfer rate or heat flux in solid structures can be calculated by known material properties such as measured temperature gradient and heat conductivity. Also, it is shown that the same concept can be used on 3D structures to get the heat flux density and heat transfer rates. [10]

2.1.2 Convection

Convection is energy transfer between a surface of solid and the adjacent fluid which is in motion. Convective heat transfer requires the combined effects of conductive heat transfer and fluid motion. In general, faster fluid motion has greater convection heat transfer. [11]

Convection heat transfer can be distinguished by two types: forced convection and natural (or free) convection. Convection is called forced convection if the fluid is forced to flow over the surface by external means such as a fan, pump, or the wind. On the other hand, convection is called natural (or free) convection if the fluid motion is cause by the variation of temperature in the fluid, which leads to the density difference. Both forced and natural convective heat transfer are illustrated in Figure 2-1. In many real-life applications, however, natural and forced convection occur at the same time. [12]

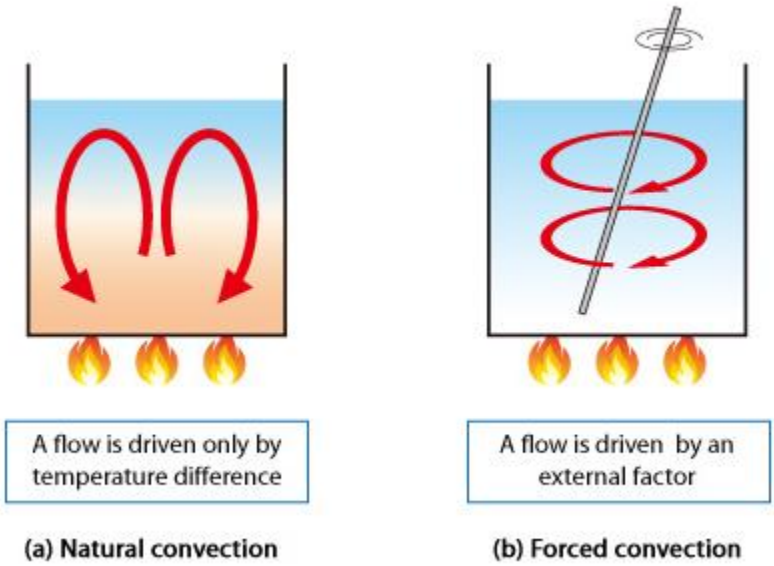

Figure 2-1. Forced convection and natural convection heat transfer [Public Domain Image]

Heat transfer by convection is not simple to analyze like heat transfer by conduction because no single property of the heat transfer medium can be used to describe the process. Convective Heat transfer depends on individual situations, and it is mostly combined with the mode of fluid flow. In practice, analysis of heat transfer by convection is treated by some factors such as fluid velocity, fluid viscosity, heat flux, surface roughness and type of flow (single-phase or two-phase). [13]

Understanding of the characteristics of the working fluid is required to understand the modes of convective heat transfer. As a result, we need to study some of the parameters in fluid mechanics which are helpful to determine the mechanism of fluids.

Among the parameters, Reynolds number has a key role to characterize fluids and it is widely used. The Reynolds number is the ratio of a fluid's inertial force to its viscous force. We can predict whether fluid flow is laminar or turbulent based on the Reynolds number. If the Reynolds number is less than 2300, the flow is laminar. Similarly, we call the fluid flow as

turbulent flow where the Reynolds number is over 4000. In between these values indicates transient flow where the flow is transitioning from one to the other.

The form of the Reynold's number can be given as:

$$Re = \frac{internal\ forces}{viscous\ forces} = \frac{mass \cdot acceleration}{dynamic\ viscosity \cdot \frac{velocity}{distance} \cdot area} \quad (11)$$

which is

$$\frac{\rho \cdot L^3 \cdot \frac{s}{t}}{\mu\left(\frac{s}{L}\right)L^2} = \frac{(\rho L^2) \cdot \frac{1}{t}}{\mu} = \frac{\rho s L}{\mu} = \frac{sL}{\nu} \quad (12)$$

where s is the maximum speed of fluid[m/s], ρ is the density of the fluid [kg/m^3], L is a characteristic linear dimension[m], t is time, μ is the dynamic viscosity [Pa $\cdot$ s or N $\cdot$ s/m^2 or kg/m $\cdot$ s] and ν is the kinematic viscosity.

The basic relationship for heat transfer by convection started with Newton's law of cooling. Isaac Newton, British physicist and mathematician, proposed this cooling law in 1701 which can define and calculate the rate of convective heat transfer between a fluid and a surface.

Differential equation of Newton's cooling law in convection is given by Fourier's law:

$$\frac{dQ}{dt} = h \cdot A \cdot (T(t) - T_{env}) = h \cdot A \cdot \Delta T(t) \quad (13)$$

where h is the heat transfer coefficient $\left[\frac{W}{m^2 \cdot K}\right]$,which depends on type of the fluid flow (laminar or turbulent), the fluid properties and roughness of the substance surface. Also, A is the area of the object through which heat is being transferred $[m^2]$ and δT is the difference between surface temperature and local fluid temperature in Kelvin. [14]

2.1.3 Radiation

Radiation is the form of energy emitted by matter as electromagnetic waves and it occurs through a vacuum or any medium (solid or fluid). As a result of random movement of atoms and molecules in substance, the charged particles emit electromagnetic radiation from the surface by carrying energy away from it. In comparison to conduction and convection, the transfer of heat by radiation can occur without an intervening medium and does not suffer from attenuation in a vacuum. [15]

Heat emitted by the matter surface depends on the surface temperature. The maximum rate of heat transfer by radiation can be expressed by Stefan-Boltzmann law as:

$$Q_{emit,max} = \sigma A_s {T^4}_s \ [W] \quad (14)$$

where $\sigma = 5.670 \times 10^{-8}$ [W/m^2 · K^4] is the Stefan-Boltzmann constant. Heat transfer rate is proportional to A_s, the radiating surface area, and ${T^4}_s$, fourth power of surface temperature.

Radiation heat transfer rate can emit at the maximum rate when the surface is a blackbody which has idealized surface. Unlike this blackbody surface, the radiation emitted by real surface is smaller than the blackbody radiation at the same temperature by using ε, the emissivity of the surface, and is expressed as:

$$Q_{emit} = \varepsilon \sigma A_s T^4{}_s \ [\mathrm{W}] \quad (15)$$

Emissivity, whose value is in the range $0 \leq \varepsilon \leq 1$,is a measure of how closely a surface approximates a blackbody for which $\varepsilon = 1$.

Understanding heat transfer by radiation is useful to investigate heating and cooling in many scientific and industrial processes. In this work, thermal radiation is used to explain the laser heating method for water temperature increase. However, conduction and convection heat transfer are mainly used to design thermal mass ToF flow meter device by using heat pulse with Tungsten wire heating method.

2.2 Thermal system analysis

In the beginning of this chapter, heat and its transfer were described in three different ways: conduction, convection and radiation. A basic concept of all three mechanism is that heat transfer happens from a high energy position to a low energy position where it makes a change of temperature in local area. From this heat transfer concept, measuring the temperature change in the measurement system is used to understand and calculate thermal time of flight measurement method.

Understanding the heat transfer which is happening inside of the temperature measurement is important for several reasons. First, we are able to predict analytical result of temperature change at our designed location. Second, it allows different experimental methods using various heat sources, device materials and fluid samples. Furthermore, studying heat transfer helps us to understand physical interaction, chemical or biological interactions.

Both device development and measurement method development are possible throughout many changes of measurement parameters and observation of heat transfer. In

this chapter, various thermal system concepts will be addressed in detail including thermal resistance, thermal mass, heat pulse and heat dissipation. Those concepts will help us to optimize our flowmeter design and its corresponding results.

2.2.1 Thermal resistance

In this work, we are interested in heat transfer rate through a medium or matter under steady conditions and boundary temperatures. The relationship between energy transfer through matter and thermal conductivity of the material can be explained by introducing the thermal resistance concept. This concept is similar to an electrical circuit where voltage, current and resistance are used. The thermal resistance corresponds to electrical resistance, temperature difference corresponds to voltage, and the heat transfer rate corresponds to electric current. Figure 2-2 shows heat transfer through two plane walls and the equivalent thermal circuit. [16]

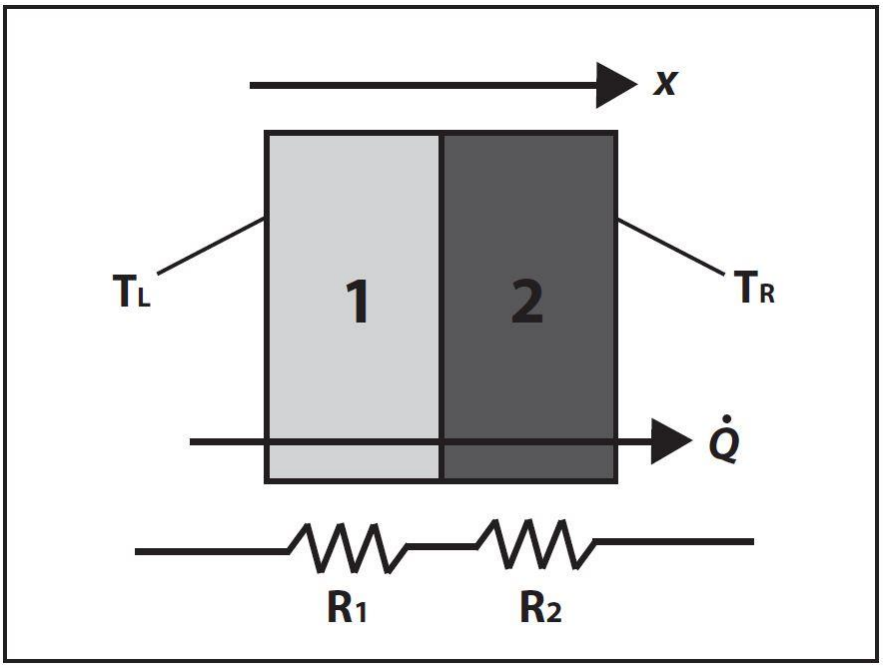

Figure 2-2. Heat transfer across a composite slab (series thermal resistance)

Energy equation for the wall can be expressed as:

(rate of heat transfer into the wall) - (rate of heat transfer out of the wall)

= (rate of change of the energy of the wall)

or

$$\dot{Q_{in}} - \dot{Q_{out}} = \frac{dE_{wall}}{dt} \quad (16)$$

In the following section, the thermal resistance equations for conduction, convection and radiation are introduced.

Fourier's law can express heat conduction for the wall as:

$$\dot{Q_{cond,wall}} = -kA\frac{dT}{dx}[W] \quad (17)$$

where $\dot{Q_{cond,wall}}$ is the rate of conduction heat transfer and A is the wall area.

In addition, thermal resistance of the wall against heat conduction can be expressed by

$$R_{wall} = \frac{L}{kA}\ [k/W] \quad (18)$$

With this equation, Fourier's law can be rewritten as:

$$\dot{Q_{cond,wall}} = kA\frac{T_1 - T_2}{R_{wall}}[W] \quad (19)$$

Electric current flow I is expressed as:

$$I = \frac{V_1 - V_2}{R_e} \quad (20)$$

where R_e is electrical resistance, and $V_1 - V_2$ is the voltage across the resistance.

By applying the same electrical concept to convection heat transfer, Newton's law of cooling for convection heat transfer rate is expressed as

$$\dot{Q_{conv}} = hA_s(T_s - T_\infty) \quad (21)$$

which can be rearranged as

$$\dot{Q_{conv}} = \frac{T_s - T_\infty}{R_{conv}}[W] \quad (22)$$

where

$$R_{conv} = \frac{1}{hA_s}[K/W] \quad (23)$$

is the thermal resistance of the surface against heat convection.

Applying the same analogy to radiation heat transfer, the rate of heat transfer between a surface can be expressed as

$$\dot{Q_{rad}} = \frac{T_s - T_\infty}{R_{rad}}[W] \quad (24)$$

where

$$R_{rad} = \frac{1}{h_{rad} A_s} [K/W] \quad (25)$$

is the thermal resistance of a surface against radiation. Here, T_{surr} is an average temperature at the surrounding surfaces.

The thermal resistance analogy concept makes the problem much easier to understand and analyze heat transfer for complicated structures. In practice and also in this work, we frequently encounter problems that consist of several layers of different materials and phenomena including different types of fluid flow. For an example, we also can apply this concept to a cylindrical shape material as in this project and develop thermal resistance equations at the boundary with the specific conduction, convection, and radiation conditions.

Fourier's law of heat conduction for heat transfer through the cylindrical layer can be expressed as

$$\dot{Q}_{cond,cyl} = -kA \frac{dT}{dr} [W] \quad (26)$$

where $A = 2\pi rL$ is the heat transfer area at location r.

This equation can be rearranged as

$$\dot{Q}_{cond,cyl} = \frac{T_1 - T_2}{R_{cyl}} [W] \quad (27)$$

where

$$R_{cyl} = \frac{\ln(r_2/r_1)}{2\pi Lk} = \frac{\ln(Outer\ radius/Inner\ radius)}{2\pi \times Length \times Thermal\ conductivity} \quad (28)$$

is the thermal resistance of the cylindrical layer against heat conduction.

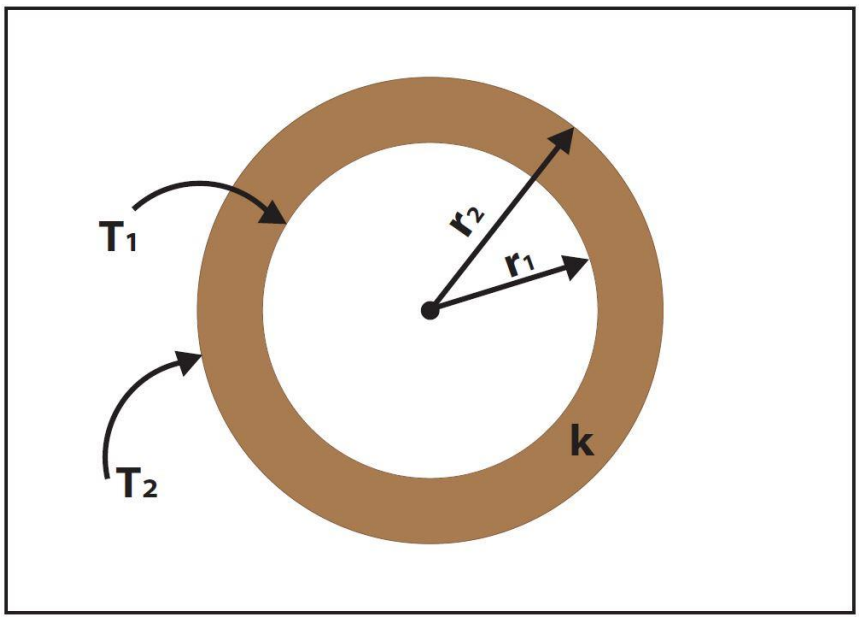

Figure 2-3. A long cylindrical pipe with specified inner and outer surface temperatures T_1 and T_2

2.2.2 Thermal mass

In device design, one of the key roles of thermal system analysis is thermal mass. Thermal mass is an ability of material to store heat energy. In other words, we often call it heat capacity which is able to act like a battery for saving heat energy.

Knowing thermal admittance values of body which is heat transfer coefficient can be useful tool to design structures. By quantifying thermal admittance, we could get material's ability to absorb and release heat change through a certain period of time. Thermal admittance is

$$h = \Delta Q / A \times \Delta T \, [W/m^2K] \quad (29)$$

where h is heat transfer coefficient, ΔQ is heat input or heat lost, A is heat transfer surface, and ΔT is difference in temperature between the solid surface and the adjacent air space.

There are three main factors which can determine the thermal mass: specific heat capacity, density, and thermal conductivity. Specific heat capacity in isobaric material can be expressed as $C_p\ [J/kg \cdot K]$. Using mass of the body m and C_p, we can define thermal mass as

$$C_p = mC_p \quad (30)$$

And from the equation of thermal energy to thermal mass,

$$Q = C_{th}\Delta T \quad (31)$$

where ΔT is the change in temperature, we can rewrite the thermal mass equation as:

$$Q = mC_p\Delta T \quad (32)$$

In this work, we concentrate on the thermal mass of fluids. In both goals of our flowmeter work, which are identifying the flowrates and the types of fluids, thermal mass has a very important role. As long as different types of fluids have different density and thermal conductivity factors, thermal mass would be different from one to another and the heat transfer rates are also different during the same amount of time through the medium.

2.3 Thermal mass time of flight method

In this chapter, new type of flowmeter measurement is introduced using thermal mass time of flight (TOF) method. As described in chapter 1, this new idea was developed from thermal mass flowmeter combined with a concept of time of flight.

Again, the basic concept of thermal mass flowmeter is utilizing the thermal properties of the fluid to measure the flow rate. Flow rates can be measured by the temperature change from the sensor for the flowing fluids. This flowmeter needs to be calibrated according to each fluid's properties before using it.

However, there are several disadvantages of using common thermal mass flowmeter. First, probes of heating elements and temperature sensors located inside the pipe can disturb fluid flow. Second, the temperature sensors and devices which need to be contacted with fluids have short or limited lifetime due to corrosion. Third, it requires large power consumption because the heating element must be continuously maintained at constant temperature value to use as a reference point. Thermal mass TOF measurement method is developed to make up for the weak points of ordinary thermal mass flowmeter.

The basic principle of time of flight is measuring time difference by calculating a travel time of signal based on the distance from the point where the signal is emitted to the desired point where we want to receive the signal. The most common sources of time of flight measurement are light and sound.

In this project, thermal mass is used as a tracer to record the time delay from one position to another position by following same principle of time of flight. The heater generates a heat pulse or pulses and the temperature sensor detects the temperature pulse after a time delay. Because the time delay of the temperature is measured, the thermal properties of the liquid/gas sample are not necessary to calculate the flow rate. Figure 2-4 and 2-5 show the principle of thermal mass TOF flowmeter.

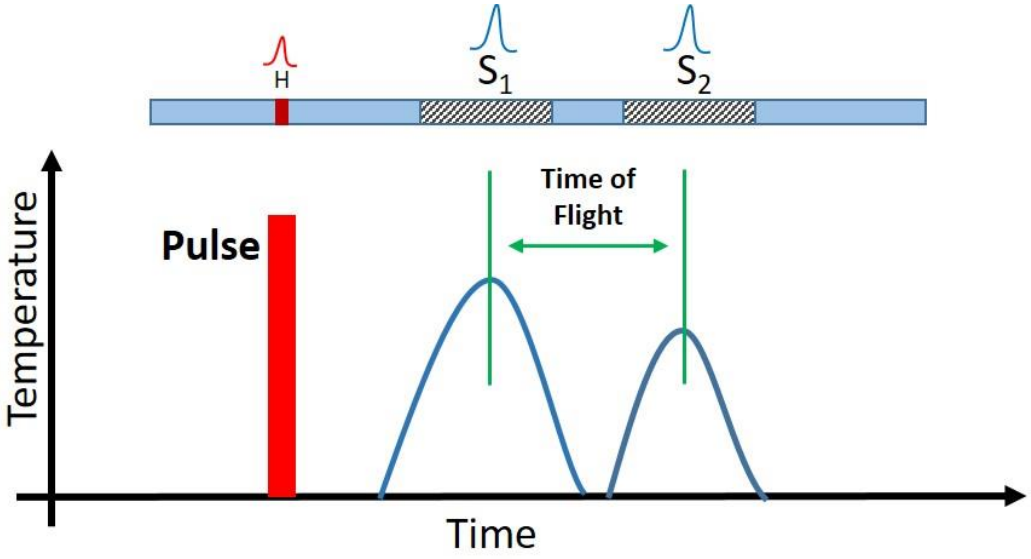

Figure 2-4. Principle of thermal mass time of flight measurement method where, H is heater and S_1 and S_2 are integrated sensor1 and sensor2 along the pipe.

We measure travel time of heat pulse from heater position to sensor1 or sensor2. In addition, time of flight can be measured between two sensors as shown in the Figure 2-5.

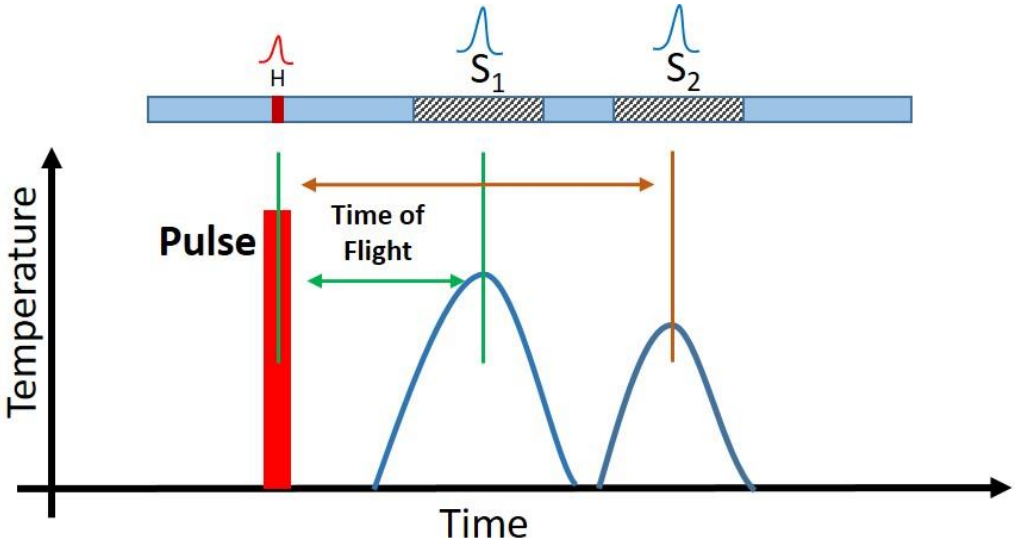

Figure 2-5. Principle of thermal mass time of flight measurement method

The main difference between ordinary thermal mass flowmeter and the new thermal mass ToF flowmeter is locations of heating element and the temperature sensor. Unlike thermal mass flowmeter, heating element and temperature sensors of new flowmeter do not contact the fluids. In addition, we are using transient power to generate heat pulse or heat pulses, rather than using a continuous power to the heating element. From the point of view of the drawbacks of ordinary thermal mass flowmeter, the flowmeter using the ToF method has less power consumption and longer lifetime of device.

2.4 Heat pulse methods

Generating thermal mass is one of the main parts of this thermal mass ToF flowmeter. It is important that we know the different types of heating elements and their principles and abilities because it is our source for the ToF measurement. Heat can be initiated by various means but there are two main methods of applying heat to fluids. First method is tungsten wire Joule heating method and the second one is the laser heating method.

2.4.1 Joule heating

Heat is produced when an electric current is passed through a conductor after some time. Some amount of electrical energy is converted into heat energy while the current is passing through the conductor. This effect is known as the heating effect of current or Joule's heating effect.

Joule, an English physicist, mathematician and brewer who studied the nature of heat, discovered the relationship between mechanical work and heat in terms of energy. He published results of experiments showing that the temperature rises from the fixed mass of water due to a known current flowing through the wire. [17]

According to the Joule's law, heat produced in a conductor due to the flow of current is directly proportional to square of the current I^2, the resistance of the conductor R, and t, the time for which the current is passed.

This heat produced energy can be converted from the total amount of work done in moving a charge q from A to B. It is given by:

$$\mathrm{W} = \mathrm{q} \times \mathrm{V} \quad (33)$$

where, V is potential difference between A and B.

Now, we know that $\mathrm{charge} = \mathrm{current} \times \mathrm{time}$ or

$$\mathrm{q} = \mathrm{I} \times \mathrm{t} \quad (34)$$

and

$$\mathrm{V} = \mathrm{I} \times \mathrm{R} \quad (35)$$

from the Ohm's law.

Putting the q and V values in equation (33) we get:

$$\mathrm{W} = I^2\mathrm{Rt} \quad (36)$$

Assuming that all the work done is converted to heat energy, heat is expressed as:

$$H \propto I^2 Rt \quad (37)$$

$$H \propto (I^2 RT)/J \quad (38)$$

where J is called Joule's mechanical equivalent of heat.

In this method using wire heating, heat starts from the wire and dissipates toward fluids through glass wall. Several parameters can be affected in the heat measurement; such as current amount, time duration of heat pulse, wall thickness, and types of fluids. Temperature change and the result of the measurement will differ according to those parameters.

In this project, tungsten wire is used as a heating element because of its proper features. In chapter 3, more detailed information for tungsten heating element will be addressed.

2.4.2 Laser heating

One of the other methods to heat up the fluids is laser heating method. The feature of the heating of a material by laser is different depending on the type of material and operating modes and conditions. Important operating conditions include the power of the laser, laser beam size and laser-pulse duration. In addition, heat by laser beam is related to the illuminated material thickness or the properties of the fluid if the material is a liquid type. There are two different ways to heat up the fluids by using this method. First, heat is generated from the fluids inside when the laser illuminated the fluids and it absorbs the laser energy. Second, laser heating on metal material also can generate temperature rise of fluid which is in contact to the materials. Laser heating method will be briefly introduced in future work section. [18]

2.5 Flow visualization with Schlieren imaging system

2.5.1 Introduction of flow visualization

The observation by visual inspection always has been used in analysis of physical process to get a successful measurement if a pattern can be observed by it. Especially in flow pattern analysis, one can get an idea of the whole development of the flow by visually observing flow patterns. Flow pattern can be developed as stationary or variable with time. They may be fully developed steady motion or complex three-dimensional eddying motion. In that sense, flow visualization has been developed in many ways and has become one of many important tools in experimental fluid mechanics.

In this section, visualization methods for compressible flows are described that lead to changes in the fluid index of refraction of the flow. The methods can provide useful qualitative and quantitative information on the spatial variations coming from the fluid density, temperature, or pressure. The methods to be described in this section include the shadowgraph and interferometry imaging techniques, especially Schlieren method. Using above techniques and principles might help to understand flow pattern in our thermal mass time of flight flowmeter and develop its performance by modifying the heating motion. [19][20]

Schlieren imaging systems have been used since the early 1800's to provide an informative method for studying transparent media. They are used to study optical media and changes in refractive index within the material. Schlieren optics have helped to visualize fluctuations in optical density. Using this method in fluid dynamics is profitable because it does not interfere with flow and it is sensitive to changes of media. As a straightforward visualization tool, Schlieren systems have been applied to visualize diverse subjects such as shock waves from a plane in flight, inhalation in humans and animals and heat burst from a system. [21][22][23][24]

Exploration of schlieren imaging has been developed with the rise of powerful digital cameras, computing power, and new strategies for studying refractive media based on Schlieren optics. As a result, these systems have value in the new application fields such as biology, physics, and environmental engineering. Using above techniques might help to understand flow pattern in our thermal mass time of flight flowmeter and develop its performance by modifying the heating motion. [25][26][27][28]

2.5.2 Optical theory

Basic concept of optical system is needed in order to understand the phenomena of these methods. Light is a form of electromagnetic radiation, which may be characterized by its wavelength or frequency, amplitude, phase, polarization, and speed, and direction of propagation. As light is transmitted through a transparent medium, any or all of its characteristics may be altered due to the interaction with the medium. This is a refraction of light. In optics, refraction is a phenomenon that occurs when light waves pass from a medium to a different medium. At the boundary layer between the media, the phase and velocity of the wave are altered causing a change in its traveling direction. Commonly, the wavelength increases or decreases, but its frequency remains constant.

Refraction in Schlieren system follows Snell's law. Figure 2-6 illustrates the Snell's law. For a given pair of media ($n_1 \; and \; n_2$) and a wave passing through them, the ratio of the sines of the angle of incidence θ_1 and refraction θ_2 is equivalent to the ratio of phase velocities v_1 and v_2 in the two media, and indices of refraction ($n_1 / \; n_2$) of the two media.

$$\frac{sin\theta_1}{sin\theta_2} = \frac{v_1}{v_2} = \frac{n_2}{n_1} \quad (39)$$

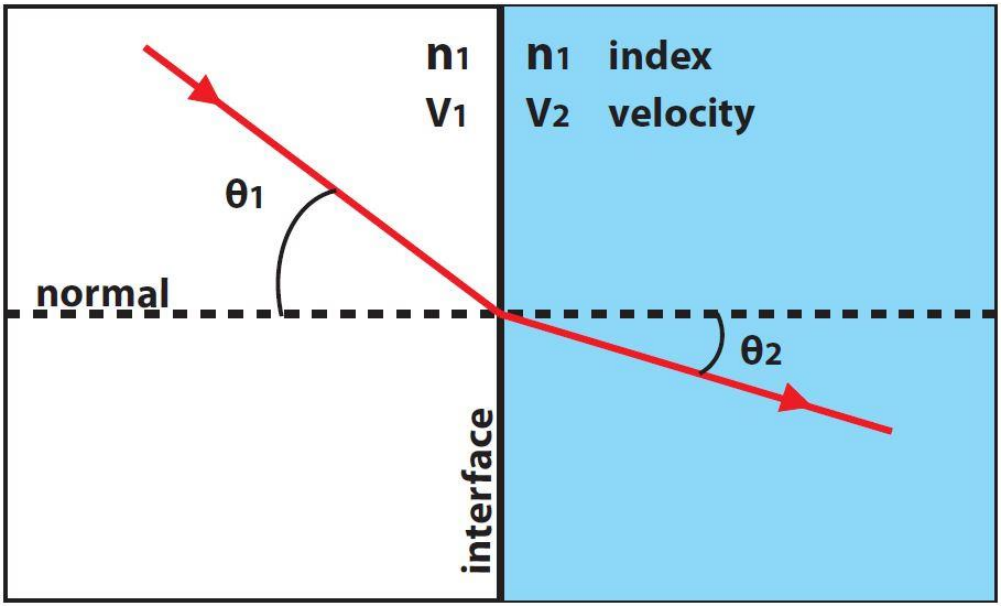

Figure 2-6. Refraction is the bending of light rays when they pass from a fast medium (rarer medium) to a slow medium (denser medium) or the opposite way. The amount of bending depends on the refraction indices of the two media and it is described quantitatively by Snell's law.

In compressible flow, light rays passing through the fluid make optical disturbance because the optical index of refraction of the fluid is a function of the fluid density. Light travels uniformly with constant velocity if media is homogeneous, such as in a vacuum. However, when the light encounters inhomogeneous media, such as fluids in motion, light rays refract or deflect. Figure 2-7 shows schematic of the deflection of light rays by different density field.

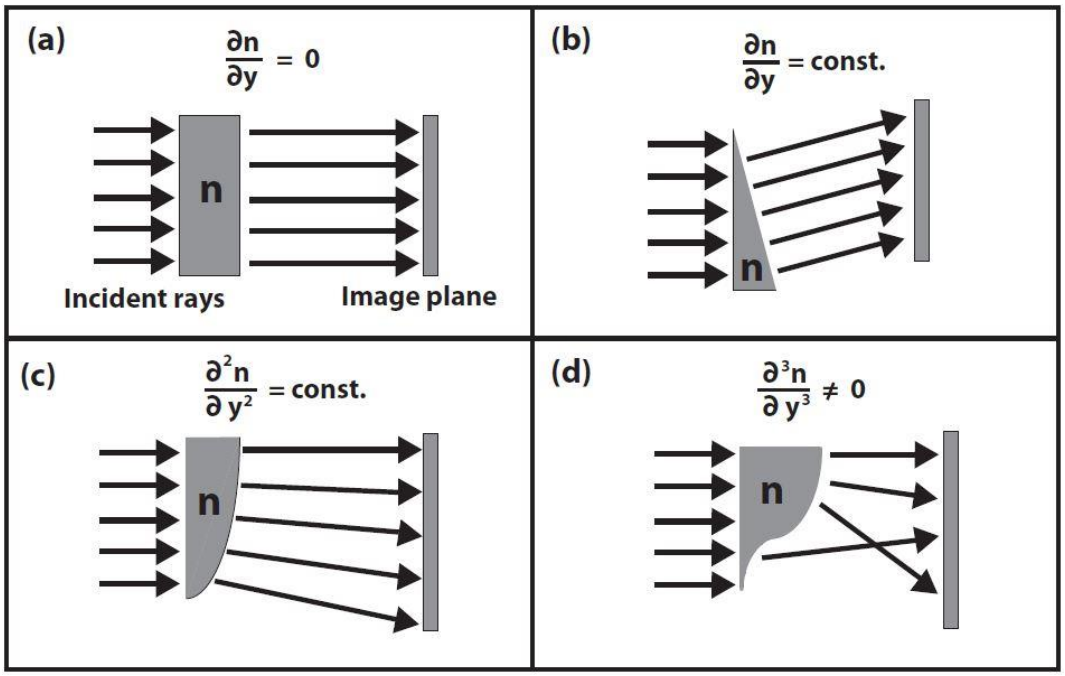

Figure 2-7. Schematic of the deflection of light rays by different density fields. Results of light rays deflection are determined by states of the first, second, and third derivative of each field (a),(b),(c), and (d).

Schlieren imaging system will visualize the density variations if the second derivative of the density is not constant. In the case of a rectangular transparent block with different refractive index as shown in the Figure 2-7 (a), the light is not deflected but the arrival time of the wave is delayed. In case of (b), where the gradient of the refractive index, $\frac{\partial n}{\partial y}$, is constant, the density has a linear variation. All rays passed through the region of the flow have the same deflection angle of the rays. Uniform light rays show up on the image plane for this region. When the region block has a constant curvature as shown in (c), the second derivative of density field, $\frac{\partial \hat{} 2n}{\partial y \hat{} 2}$, is constant. Illuminated light rays also show a uniform pattern on plane surface although the size of image is different. As a result, the shadowgraph techniques visualize fluctuation of sample region only when the density field has non-uniform $\frac{\partial \hat{} 2n}{\partial y \hat{} 2}$ which means that $\frac{\partial \hat{} 3n}{\partial y \hat{} 3} \neq 0$ everywhere. [19][20]

The most fundamental schlieren system needs a straight-line arrangement of lenses to visualize Schlieren imaging as shown in Figure 2-8. First, a parallel light beam is emanated from a light source, E, passed through slit, O, and focused by collimating lens, L1. This parallel beam is then deflected by the test media F and passed through a second lens, which is Schlieren lens, L2. Then, beam is focused on the knife-edge, K, and collected by focusing lens, L3. From L3, the Schlieren image is projected onto a flat screen surface, H.

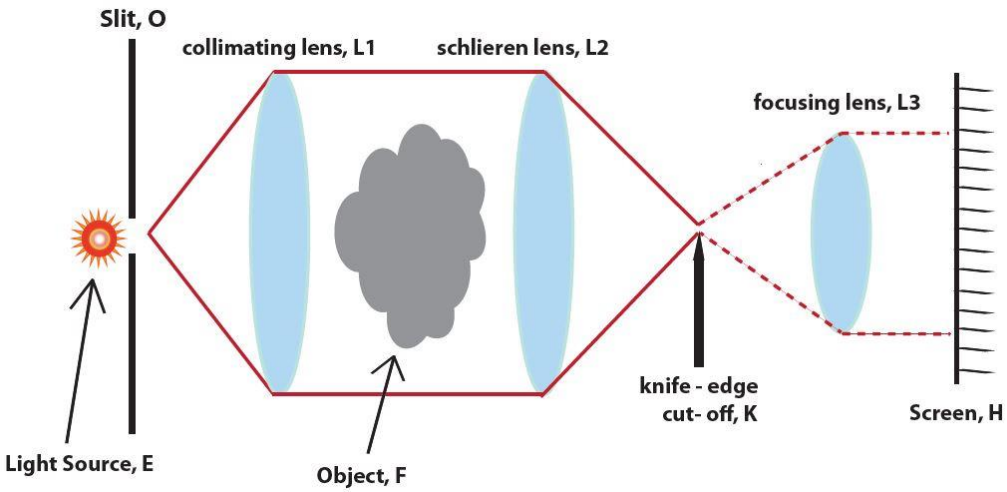

Figure 2-8. A typical setup of Schlieren optics system

2.5.3 Related systems

1. Shadowgraph

Shadowgraph is a type of flow visualization and related to the Schlieren method that perform a similar function, but it is simpler. In principle, we cannot directly see a temperature difference or a shock wave in the transparent medium. However, all these disturbances can refract light rays. Shadowgraph is an optical technique consisting of a light source and a viewing plane. Shadow grams which are caused by light source are projected onto a flat screen for observation. For example, the shape of hot air rising from a fire can be seen by its

shadow. In this example, parallel light source is the uniform sunlight and a screen is a flat surface nearby fire. Advantage of this method is that the shadow grams can be magnified according to distance between the object and the screen because they are simply shadows of objects. [21][23][29]

2. Interferometry

Schlieren interferometry techniques are another visualization method to be discussed in this section. Although this technique is closer to interferometry than Schlieren imaging, it uses similar visualization techniques. Schlieren interferometry has given rise to more informative methods of visualization measurement since it can be applied to some form of quantitative analysis in optics. The typical setup of Schlieren interferometry is same as two-lens Schlieren imaging system, but the knife-edge is replaced with prism or fine wire to make interference or diffraction before the light rays are projected on a plane. Color Schlieren interferometry uses a color filter rather than the cut-off. In this case, diagnostic technique through Particle-Image Velocimetry (PIV), an optical method of flow visualization, is used to get quantitative data from Schlieren images. [21][30][31]

Chapter 3 Device design and fabrication

In this work, we investigate the ability of thermal mass ToF measurement flowmeter for different flow measurement application. This chapter introduces several design structures for flow measurement and methods for the designed device fabrication. This chapter will also cover the operational principle for each device component and theoretical background.

The brief information of heat transfer phenomena described in the previous chapter is used to get ideas for device design. The choice of device components mainly depends on the concept of thermal measurement. Heating element is used to apply heat pulse and RTD sensors are used to measure temperature changes. In this chapter, two different types of flowmeters are introduced based on physical size.

In this project, we designed and developed two main types of thermal flow meters with the capability to measure a wide range of flow rates. First, we fabricated a flowmeter in micro level by using micromachining techniques. This micro-fabricated flowmeter is suitable to measure very low flowrate range such as micro or nano liter per minute. This micro flowmeter is also used in microfluidic applications. The second type of flowmeter is for high flowrate range, more than 1ml/min. Each component of this macro size flowmeter will be introduced in this chapter by presenting their operation principle and material properties.

3.1 Micro-fabricated flowmeter

For applications that require the precise measurement of small flow rates, on the order of nl/min to μl/min, a micro-machined MEMS-based flow meter has been developed. The flow meter consists of two thermal elements (a heater and a temperature sensor), a microfluidic channel, and electrical interfaces integrated on a silicon chip. Resistive Temperature Detector (RTD) is used as the temperature sensor which has a resolution of 1 mK. So, it can be used for determination of extremely low flow rate (~nl/min). The RTD

sensor is made of nickel metal, and it is deposited on top of the substrate using thermal evaporation.

3.1.1 Device design & operation principle

The design of this micro-fabricated flowmeter device is based on the intended application for measuring very slow flowrate of liquid samples. Time of Flight measurement method using heat source needs several main elements to measure fluid flowrate. This flowmeter includes a fluid channel to make flow possible over a silicon chip where heater and sensor are integrated. As we described earlier in chapter 2, well-developed fluid should cross over the heating element and temperature sensor in order. Microfluidic channel provides a travel route for liquid samples. We used two different microfluidic channels for the fluids used in this project. We designed PDMS and polymide channels. Micro machined metal wire is used in this flowmeter as both heater and sensor by using metal evaporation technique and chemical etching method. Device fabrication including channel and sensor will be introduced in the following section. The basic schematic of the micro flowmeter is shown in Figure 3-1 and Figure 3-2.

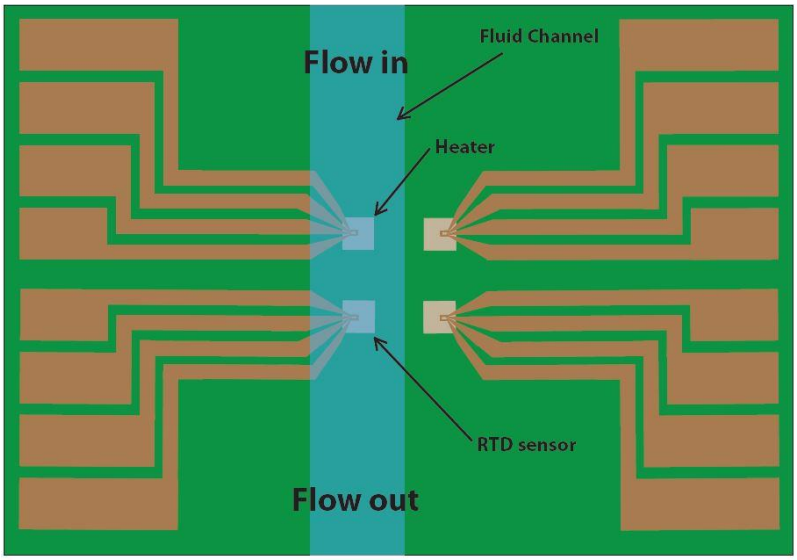

Figure 3-1. Schematic of the micro-fabricated flowmeter and configuration of flowmeter working principle. Silicon chip flowmeter device is described in 2-D model.

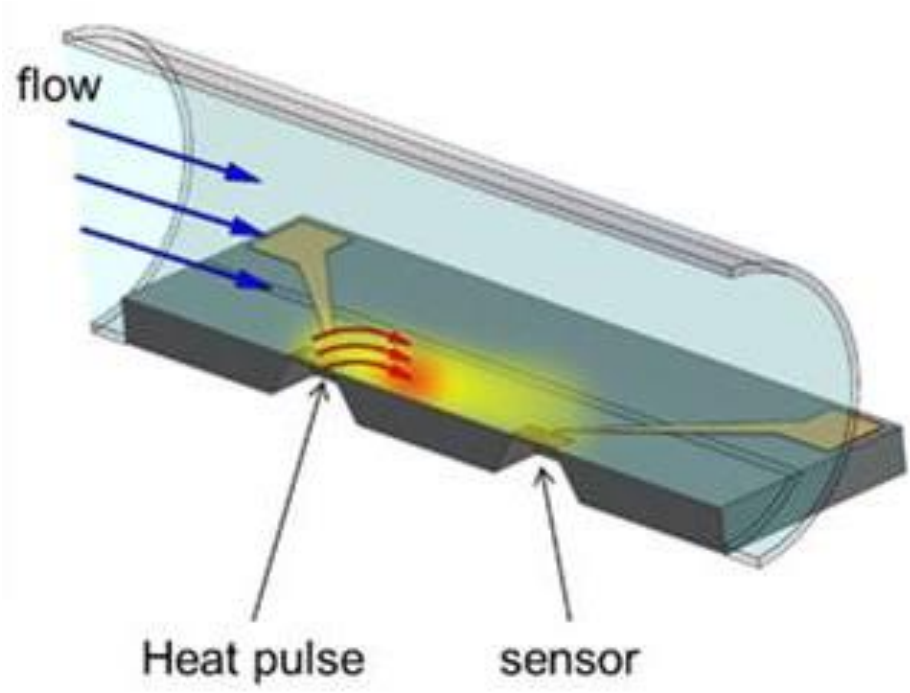

Figure 3-2. 3-D model of micro-fabricated flowmeter.

In this work, sensitivity of temperature measurement is a determining factor, which indicates the performance of this flowmeter device. Thin metal film made of Nickel is used as

a resistive temperature detector (RTD) sensor, which has a resolution of 1mK. In the case that even higher sensitivity is required, various other materials can be used, such as platinum and polysilicon. More detailed information of thin metal film RTD sensor will be introduced in the following section. This RTD sensor is integrated on a SiN membrane surface, which can help the sensor to stand on the stable substrate. Main advantage of using SiN membrane is that the thin substrate provides thermal isolation area from the silicon bulk. In Figure 3-3, real silicon chip flowmeter device is presented.

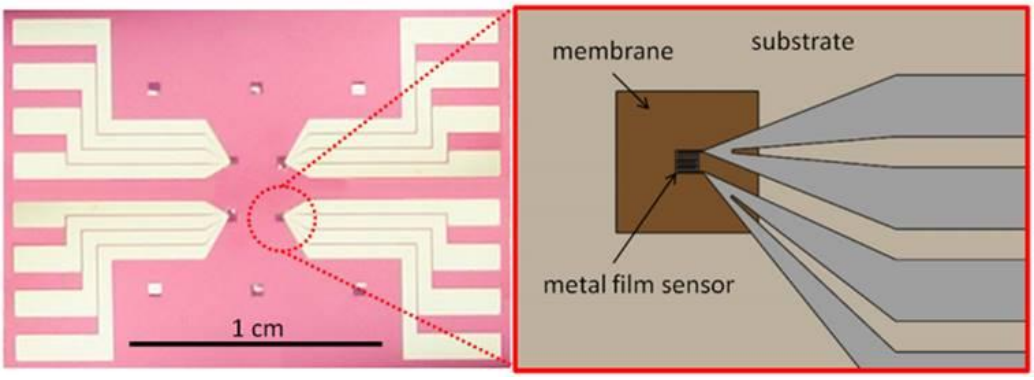

Figure 3-3. Micromachined RTD sensor which is integrated on top of the SiN membrane.

3.1.2 Micro-fabrication of flowmeter device

Micro-fabrication covers several manufacturing processes with a silicon wafer. In general, there are deposition, lithography, and etching processes. This chapter will present brief introduction of micro fabrication techniques that are related to our flowmeter device. The micro-fabricated flowmeter fabrication processes include three main parts; SiN membrane, RTD sensor, and microfluidic channel fabrication. Overall process of silicon chip micromachining is illustrated in Figure 3-4.

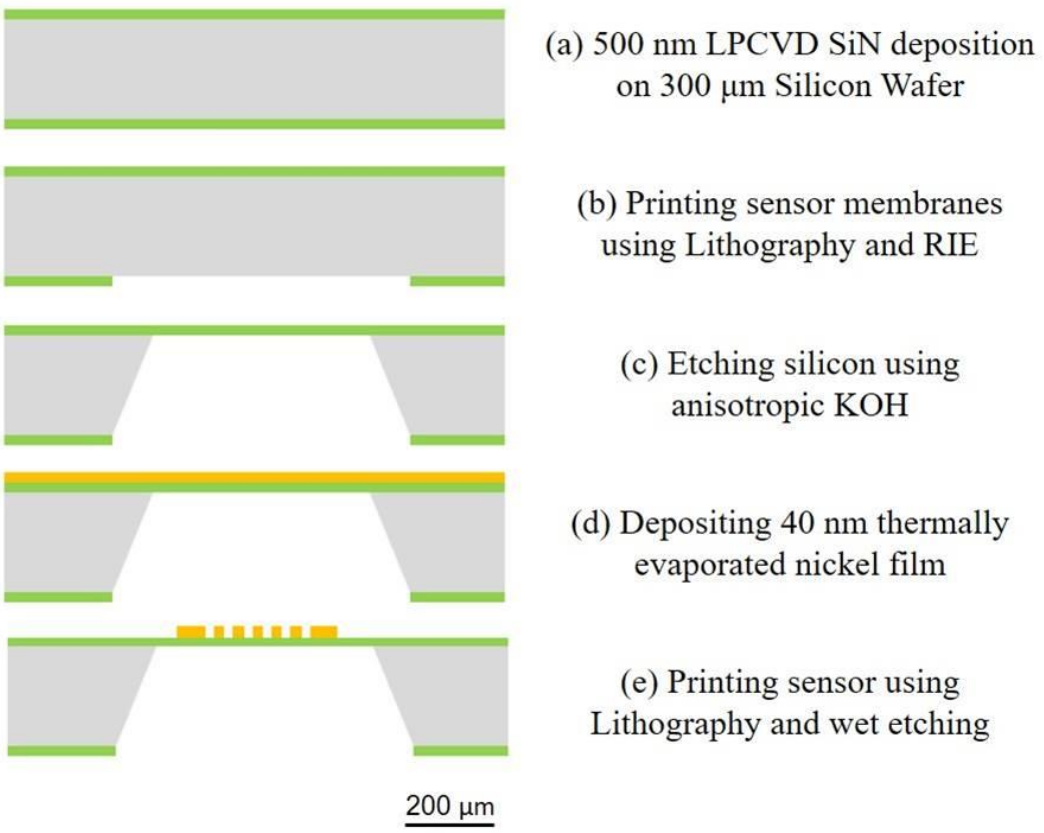

Figure 3-4. Overall process of silicon chip micromachining

Silicon chip with 300μm thickness is used as substrate of flowmeter device in this project. For many mechanical and electrical sensor applications, single-crystal Si wafers are used because of their intrinsic mechanical stability and the feasibility of integrating electronics on the wafer. Capability of micromachining with silicon makes possible to use as a substrate model even though it is high cost material.

Silicon is also used due to its extreme flatness, which can help well-established layer coating procedure. As shown in Figure 3-4 (a), thin layers of Silicon Nitride (SiN) (500nm) are deposited on both sides of Silicon wafer. Silicon nitride is used in micro sensor fabrication because it has many superior chemical, electrical, and mechanical properties. In this work, SiN thin layer plays a role of thermal insulator as membrane shape.

There are several deposition techniques, but we used Chemical Vapor Deposition (CVD) technique to deposit SiN layer on the substrate. In general, deposition is performed in vacuumed chamber and gas phased deposited material is delivered to Silicon wafer surface. In case of CVD process, deposition is based on chemical reactions between substrate and reactant gas. Low Pressure CVD (LPCVD) is utilized in our silicon chip fabrication. Using LPCVD can increase deposited film growth velocity and enhance the diffusivity.

Next step (b) shows printing technology using photolithography method. This method is a technique that can transfer a pattern onto the surface of desired layers or substrate. The steps for making membrane pattern are listed below.

1. *Surface cleaning*
2. *Barrier layer deposition*
3. *Spin coating with photoresist (PR)*
4. *Soft baking*
5. *Mask alignment*
6. *Exposure*
7. *Development*
8. *Hard Baking*
9. *Post process cleaning*

After all the steps of photolithography, desired pattern is transferred onto silicon nitride layer surface and the patterned area is ready to be etched. Then, the SiN layer is etched by Reactive Ion Etching (RIE) process.

Step (c) illustrates silicon etching process using potassium hydroxide (KOH). The silicon is etched by KOH with anisotropic wet chemical method. Because of its bonding structure, single-crystal silicon has a unique wet etching profile. {111} planes of silicon wafer

have higher density at atomic structure than other planes and KOH liquid solution etches silicon in trapezoid shape as shown in the Figure 3-4 (c). This etching process removes the silicon from the patterned SiN layer all the way to the opposite side of SiN layer and keeping the membrane at the top of the wafer.

In the next step, a 40nm thickness of nickel film is deposited on top of the SiN layer to integrate RTD sensors and heating elements. Metal evaporation technique is used to deposit thin layer of nickel film. Detailed information for metal evaporation process and its principle will be introduced in macro-fabricated flowmeter section of this chapter. Second photolithography process is performed after step (d). Using the nickel etchant helps to remove excess metal parts. The RTD sensors remain on top SiN membrane as shown in Figure 3-4 (e).

Fabrication of microfluidic channel is important part of flowmeter device design. Fluid channel can be chosen by considering two factors. First, material properties should be considered. The properties include mechanical properties, chemical stability, and thermal resistivity. Channel materials should not impinge on quality of liquid sample when they contact each other. The second matter is stability of microfluidic channel. Fully developed flow should be continuously maintained during the measurement without having leakage or bubbles. Flow control is essential to this thermal mass ToF measurement because it is directly related to heat transfer from heater site to temperature sensor.

We use two microfluidic channels using different tubing materials and methods. These two channels are illustrated in Figure 3-5. First method is using PDMS (polydimethylsiloxane) and PTFE (polytetrafluoroethylene) teflon tubing. PTFE tubing is used as a pipe line to guide liquid sample and integrated on top of RTD sensors. It has great properties including transparency, chemically inert, and non-toxic material. Due to its high flexibility, PTFE is selected to make smooth liquid channel which can generate constant flowrates. PDMS is used to secure PTFE tubing on our microchip flowmeter device. By

pouring the mixed elastomer resin and hardener on top of the tubing, it is ready to become a cured channel.

Second method is using polyimide material. Using polyimide has advantage from its properties. It is known for good chemical resistance, thermal stability, and great mechanical properties. In this project, patterned polyimide tape is attached on the surface of silicon chip. Then, microfluidic channel is made by covering the tape using thin glass cover. Two glass tubes are integrated through silicon wafer so that they can be used as flow inlet and outlet.

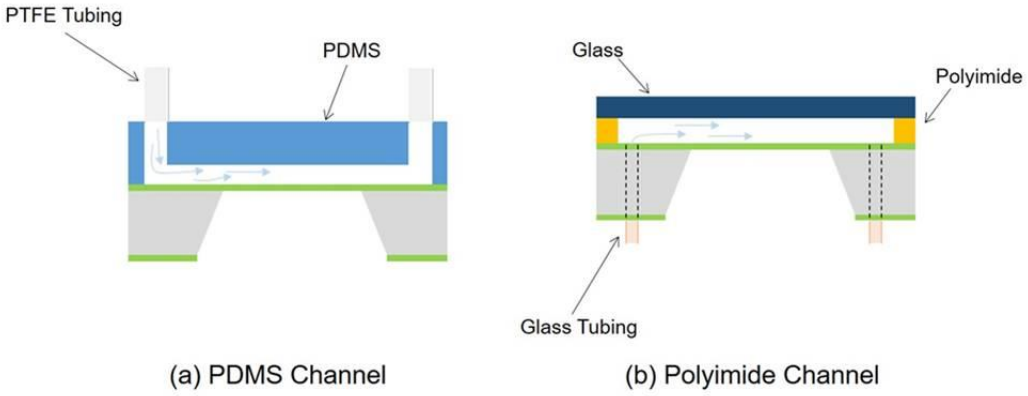

Figure 3-5. Microfluidic channels sensor which is integrated on top of the SiN membrane with two different methods (a) and (b).

3.2 Macro-fabricated flowmeter

As we discussed in micro-fabricated flowmeter section, flowrate range at microfluidic scale is low and it is difficult to use the flowmeter for other applications such as wastewater, chemical, pharmaceutical, food and beverage industries. In those applications, the other scale of flowmeter is needed so that it can manage the higher flowrate range than micro level. Design purpose of the macro size flowmeter is for higher flowrate range and we especially focused on the flowrate range from 1ml/min to 10 gal/min.

3.2.1 Device design

The operational principle of this macro-fabricated flowmeter is exactly the same as the micro-fabricated flowmeter using thermal time of flight method. This device also contains heating elements and temperature sensors. Instead of fluid channel at micro flowmeter, however, macro flowmeter uses glass capillary for flowing fluid pipe.

3.2.2 Device components

1. Glass capillary

In this project, a thin glass capillary is used as a liquid flowing pipe to conduct thermal time of flight measurement. Inner diameter of this thin glass capillary is 1.15mm and the thickness of this tube is 0.35mm ± 0.05mm. In addition, the length of the capillary is 75mm ± 1mm and the tube has a volume of 75μl. Glass can successfully carry out this measurement due to its poor electrical conductivity and it has enough thermal conductivity to transfer heat from the outside of glass tube to the inside fluid.

2. Heating Element

For the heating element, tungsten (W) wire is used. As we discussed before in chapter 2, the technique used here is the rapid Joule heating of thin metal wires. In our work, a 1A heat pulse is applied to the metal wire for 1s, 0.7s, 0.5s, and 0.3s. The reason for using tungsten wire is because it is a well-known high-temperature refractory metal. Tungsten wire can be sustained at high temperature which shows its great hardness and it has very high melting point (3,422 ± 15℃).

Electrical conductivity of tungsten is good, about a third of that of copper, as well as the thermal conductivity, which is about 43% that of copper. Uncommonly low specific heat of tungsten and its high thermal conductivity helps to heat up and cool down the metal very

quickly. Due to those temperature and electrical properties, tungsten is an ideal material for high temperature applications; such as cathode-ray tubes, vacuum tube filaments, light bulbs, heating elements and rocket engine nozzles. [21]

In this macro-flowmeter device, 70μm tungsten wire is used as a heating element. To heat up the water inside of a glass capillary, we wind one turn of tungsten wire on a surface of the capillary. Also, we put thermal compound around the interface between tungsten wire and the surface of glass capillary in order to maximize heat transfer.

3. RTD sensor

The two most common temperature sensors used for thermal mass flowmeter and industrial applications are resistance temperature detectors (RTDs) and thermocouples. Both temperature sensors have their advantages and disadvantages and we can use either device according to the application. A thermocouple has a wide range of temperature from -180 to $2{,}320℃$ compared to an RTD sensor which has a temperature range of -200 to $500℃$. In addition, the cost of thermocouples are 2.5 to 3 times less than RTDs. However, RTDs are superior to thermocouples in many other ways such as: high accuracy, repeatability, stability, less complicated fabrication, and linearity.

Metal	Relative Conductivity (Copper = 100% @ 20℃)	Temperature Coefficient of Resistance (Ω/℃)
Annealed Copper	100%	0.00393
Gold	65%	0.0034
Iron	17.70%	0.005
Nickel	12 to 16%	0.006
Platinum	15%	0.0039
Silver	106%	0.0038

Table 3-1. Temperature coefficient of common RTD metals

The basic operation principle of RTD sensors is that the electrical resistance of metals change with temperature. Even though any kind of metal can be used for temperature sensing in theory, metals with high melting points and high resistivity are chosen in practice. Table 3-1 shows different materials of RTD sensors and their properties. Gold and silver have relatively low resistivity that makes the measurement difficult. Copper has low resistivity but is sometimes used because of its low cost. The most commonly used RTDs are made of either nickel, platinum, or nickel alloys. Among those materials, platinum is the most common RTD metal, mainly because of its high resistivity and long-term stability. However, we use nickel as our RTD sensor due to its cost-effective feature and it needs low temperature to evaporate.

There are two main types of RTD sensor: wire wound type, and thin film type. Wire wound RTDs are made by winding a fine strand of metal wire into a coil shape around an insulated material. Although the wire wound RTDs are very stable, the thermal contact between the wire and the measured point has a problem. On the other hand, thin film RTDs are made by depositing a thin layer of metal on the surface of the non-conductive material. Thin film RTDs have the advantages that they provide a fast thermal response, are less sensitive to vibration, and they cost less than the wire wound sensor.

Every metal has a resistance and it is proportional to length and resistivity of the metal and inversely proportional to the area of its cross-section as shown in equation (40).

$$R = \rho L/A \quad (40)$$

where R is the resistance, ρ is the resistivity, L is the metal length, and A is the area of metal's cross-section. The resistivity increases as temperature increases as shown in (41)

$$\rho_t = \rho_0[1 + \alpha(t - t_0)] \quad (41)$$

where ρ_t is the resistivity at temperature t, ρ_0 is the resistivity at a room temperature, and α is the temperature coefficient of resistance. By setting t_0 to 0℃, we get (42).

$$\rho_t = \rho_0[1 + \alpha t] \quad (42)$$

From (40), we can write (43) and (44) as below

$$R_0 = \frac{\rho_0 L}{A} \quad (43)$$

and

$$R_t = \frac{\rho_t L}{A} \quad (44)$$

By inserting (42) into (44), we can re-write (42) as shown in (45)

$$R_t = \rho_0 \frac{[1 + \alpha t]L}{A} \quad (45)$$

and from (43) and (45), the relationship between the resistance and temperature can be written as

$$R_t = R_0[1 + \alpha t] \quad (46)$$

In this work, 50nm nickel film is deposited on the surface of a glass capillary with thermal metal evaporation equipment. Thermal evaporation or vacuum evaporation is a

common method of thin film deposition and it is widely used in micro fabrication laboratories and in industry. As shown in Figure 3-6, evaporation begins in a vacuum state, where there are no vapors other than the source material. A diffusion pump makes the vacuum chamber reach 10^{-7} torr backed by mechanical pump. Nickel at the tungsten basket can be heated by high current (30~40 A) and the Ni vapor is generated. In high vacuum, the vapor can travel directly from the basket to the substrate without colliding with non-source gas. Condensing of source vapor at the surface of target makes Ni film back to solid state and the thin film of Ni becomes RTD sensor.

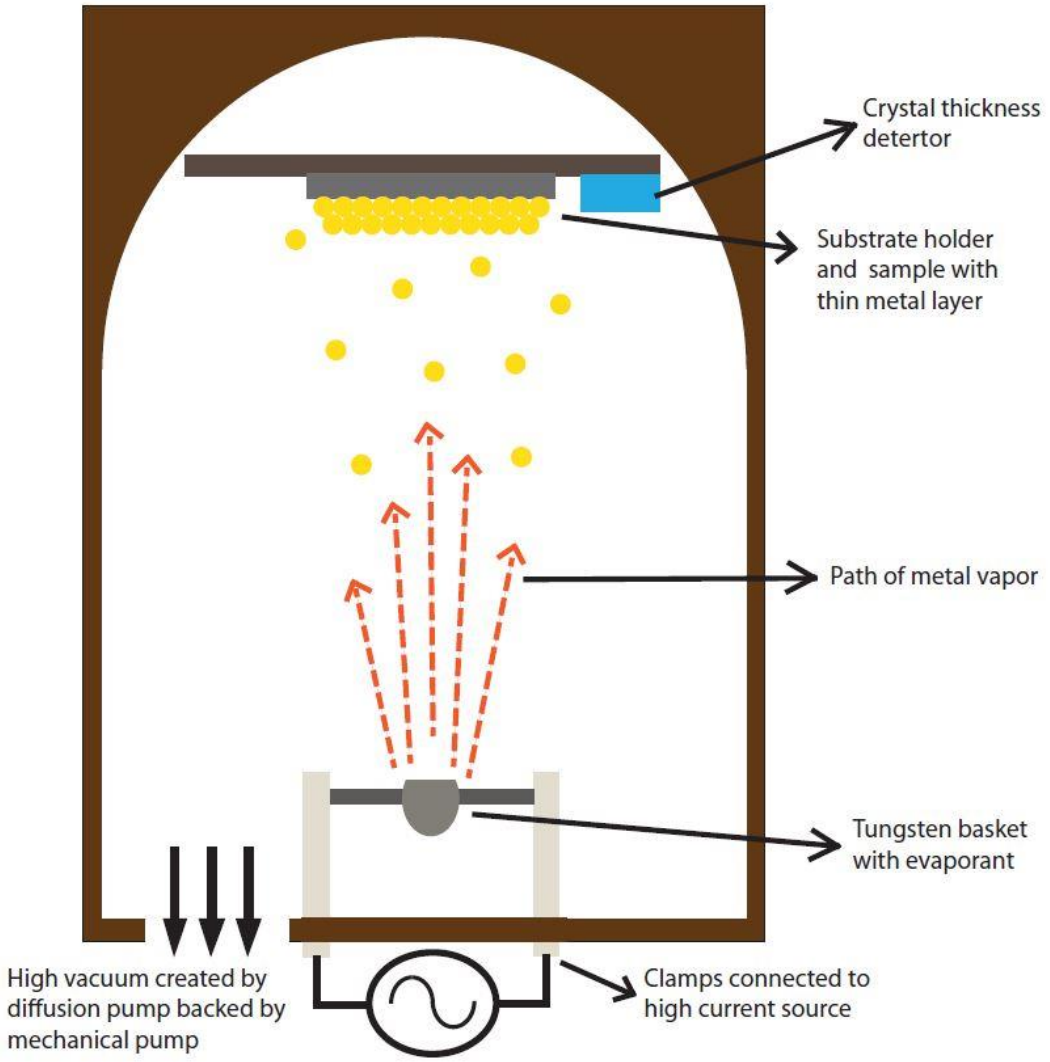

Figure 3-6. The basic configuration of metal evaporation and shadow mask

A shadow mask is designed for Nickel film fabrication to generate the pattern of RTD sensors. It helps to make accurate self-alignment and gap control between each Ni film sensor. Uniform dimension size and thickness of RTD sensors can be created by locating this shadow mask under the glass capillary as shown in Figure 3-7. A total of 19 glass capillaries can sit on the wafer slit and become the flowmeter sensors at the same time. One of the great advantages of using this shadow mask method is that we are able to reuse the mask several times to get the same sensor properties for each RTD.

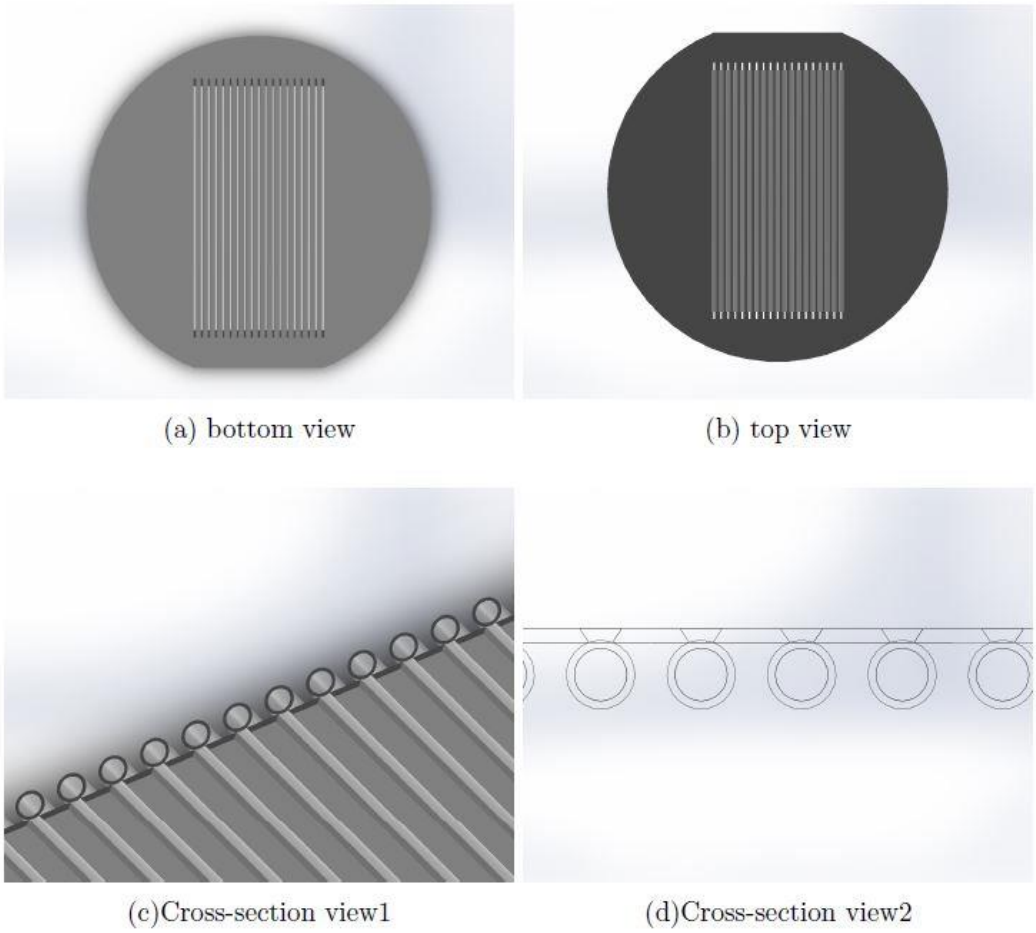

Figure 3-7. Shadow mask for RTD sensor fabrication. Glass capillaries are sitting on slits of shadow mask.

Four RTD sensors are deposited on one glass capillary as shown in Figure 3-8. Size of the RTD, or sensor length, is 3.5mm and the distance between two sensors is 8mm from center to center. Additionally, we deposited Ni film on the glass capillary to mark a location for the heating element site.

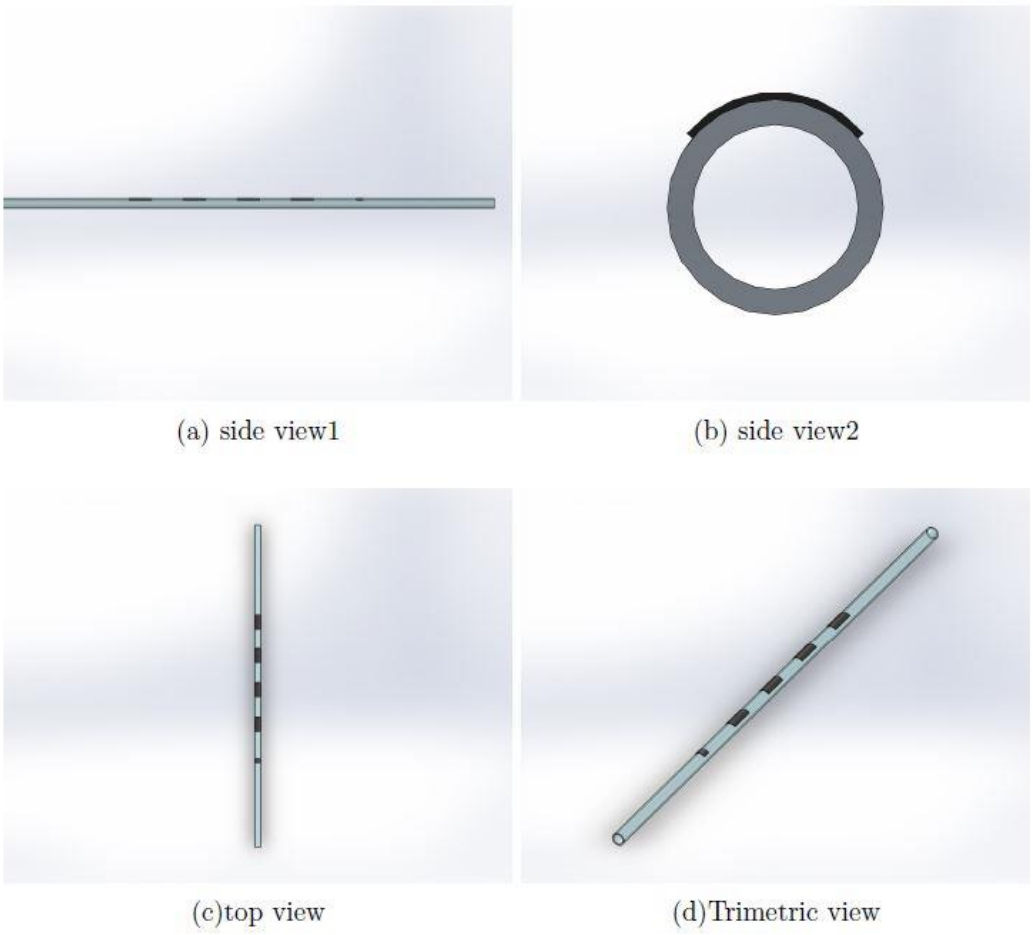

Figure 3-8. Overall view of glass capillary. RTD sensors are integrated on the surface of it.

Copper wire is used for electrical readout from the RTD sensor and we put conductive epoxy on the contact point of the wire and Ni film. Figure 3-9 shows the acrylic holder to hold glass capillary so that we can use the device in stable condition.

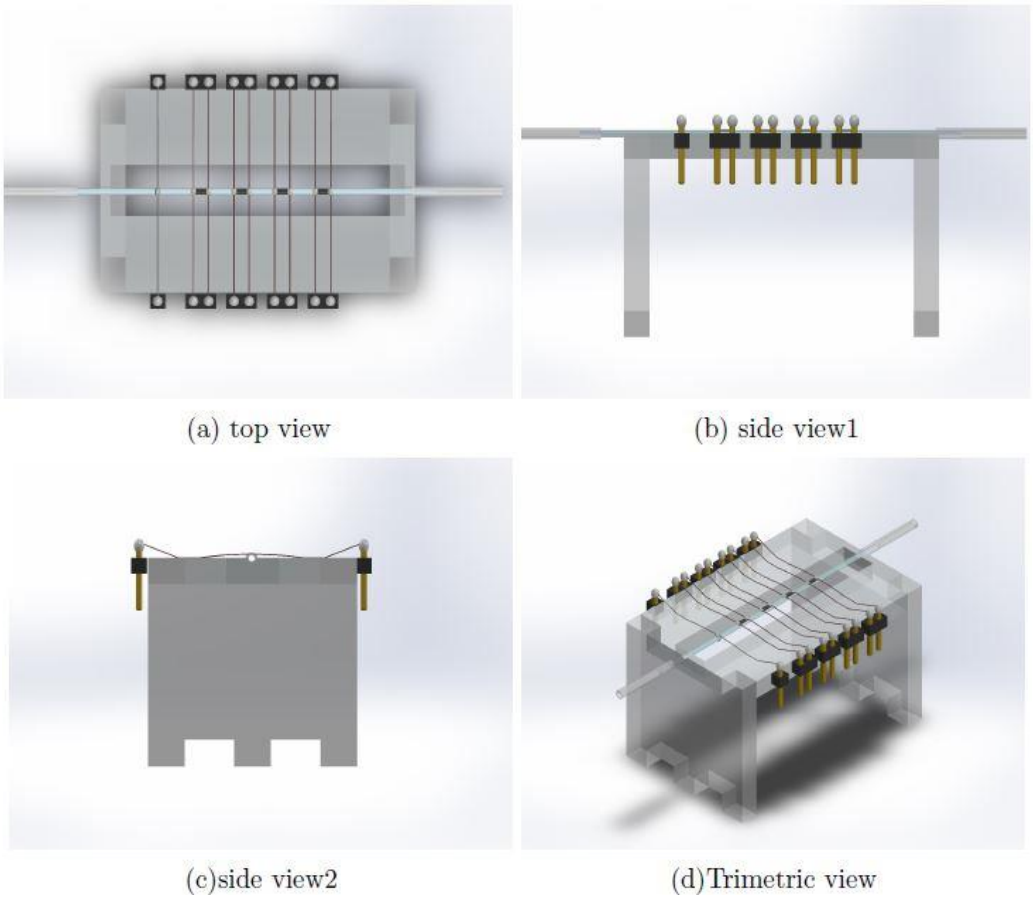

Figure 3-9. Interface setup for temperature measurement including glass capillary, RTD sensor and header pin for wire connection.

4. Bypass system

Time of flight measurement at low flowrate which is at milliliter range has no problem to get a stable data result. However, in the case of high flowrate range (higher than 1GAL/min), it is difficult to catch the temperature change from the sensor because of the high fluid velocity. The reason is that measuring time of flight of a heat pulse is not stable and detectable with high velocity. In order to get rid of the above problem, the idea of integrating bypass system was used.

As shown in Figure 3-10, we can make a pressure drop inside of the bypass pipe by using the orifice which is located in the middle of the pipe. We have orifices with 8 different

diameter sizes and each orifice is able to make different pressure drop. We can shift the measurable flow rate range up or down by changing the orifices.

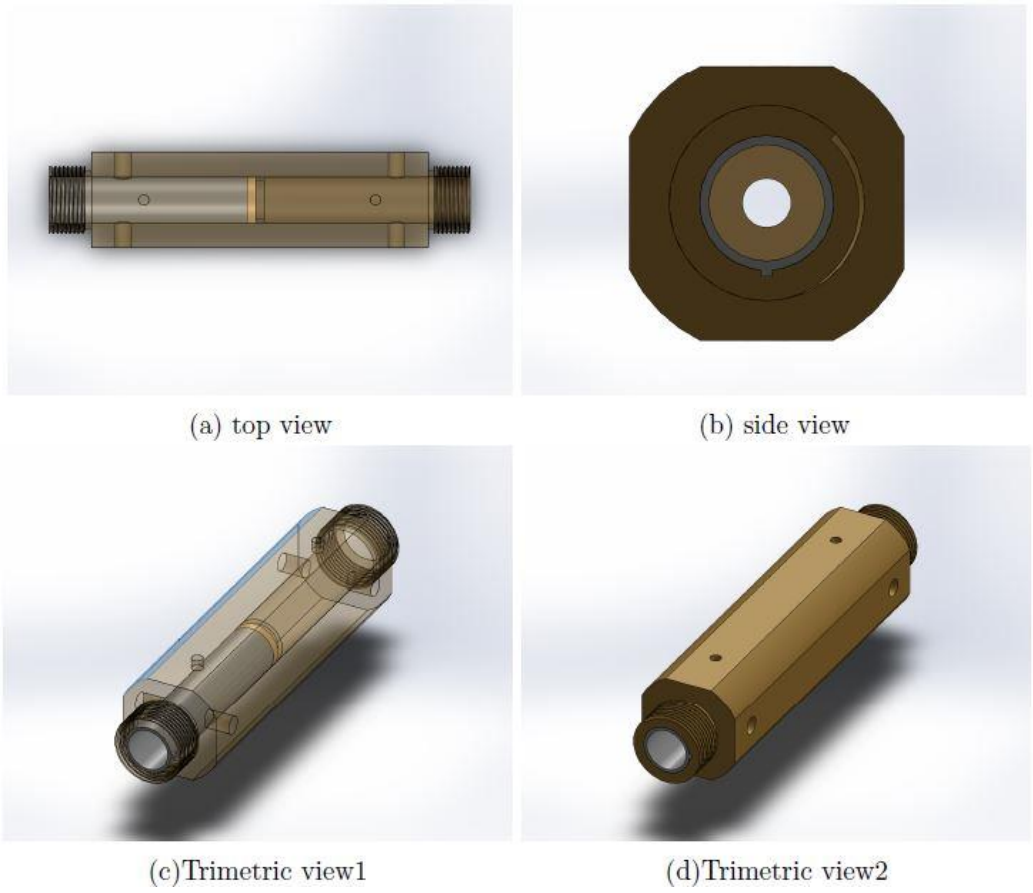

Figure 3-10. Overall view of bypass system

Chapter 4 Experimental methods and results

In this chapter, the experimental setups and results are presented for overall flow measurement using thermal mass ToF (Time of Flight) method. First, this chapter covers flow calibration system to carry out flow measurement. Then, device test and sensor optimization are discussed. After that, time of flight measurement is introduced with thermal measurement. Each section independently has their setup configuration, data results, and discussion.

4.1 Flow measurement platform

Inferential flowmeter, introduced in chapter 1, measures flow rate indirectly and cannot calculate flow rate right away without device calibration. Thermal mass time of flight method flowmeter also uses thermal energy as an indirect tool for flow measurement. It means that it needs flow calibration process to use as a product.

Knowing definition of calibration is helpful to understand the process of using flowmeter. Calibration can be defined as:
"The set of operations that establish, under specified conditions, the relationship between values of quantities indicated by a measuring instrument or measuring system and the corresponding values realized by standards." [33]

Calibration of measuring instruments is mainly used for two reasons: First, it verifies the accuracy of the instrument. Second, calibration decides the traceability of the measurement. For these reasons, it is important to use precise calibration system. There are some factors that need to be considered when we choose calibration test bench such as repeatability, reproducibility, and resolution. The resolution of the calibration must be adequate to cover measured instrument. In addition, the way the fluid interacts with the sensor can highly affect the measurement; Calibration system should establish predictable and

reproducible flow profile. Properties of the fluid such as temperature and pressure also need to be controlled in a calibrating process. [34]

Thermal mass ToF flowmeters have been developed to measure two different flowrate ranges, from 1ml/min to 10ml/min and from 1 GPM to 10GPM. As we discussed in this chapter, calibration system must generate similar flowrate range compared to the tested flowmeter. As a result, we use two different liquid flow calibration systems, BadgerMeter water calibration system and gravity driven flow calibration system. Those two systems work as our test benches, working principles and performances of them are introduced in this section.

4.2 Flowrate measurement at high flowrate

In this section, overall information about flowrate measurement at high flowrate (from 1GPM to 30GPM) is discussed. The section starts with sensor optimization of flowmeter device and detailed experimental setup. The results will follow.

4.2.1 Flowmeter optimization

The aim is to investigate how temperature sensor is accurately affected by thermal mass in the form of heat pulse packets. RTD (Resistance temperature detector) sensor detects temperature changes from the surface of glass capillary when heated water passes through the location where the RTD sensor is located. Temperature change is converted to resistance change and time of flight analysis is performed based on the resistance change profile. It is difficult to measure ToF from resistance change profile if the profile fluctuates. Sensor optimization is one process for better data analysis. At the same time, it contributes to increasing the accuracy of the flowmeter.

Many different factors affect the signal profile of resistance changes. Basically, the resistance change depends on the heat transfer and diffusion in flowing liquid and the main

factors are related to the shape of sensor (thickness or length) and location of heater and sensors. Table 4-1 shows the parameters for sensor optimization experiment and different values which we have used.

The same amount of heat pulse and flow rate is applied for every measurement for different variables and values shown in Table 4-1.

Parameter	1st	2nd	3rd
Ni Thickness	20 nm	30 nm	40 nm
S_1 Length	5 mm	10 mm	15 mm
S_2 Length	5 mm	10 mm	15 mm
S_1-Heater Distance	2 mm	5 mm	8 mm
S_2-Heater Distance	10 mm	13 mm	16 mm

Table.4-1 Sensor optimization variables

From sensor optimization, we found relationships between sensor parameters and temperature change profiles. First, sensor length is related to the width of peak function. As the sensor length gets wider, the time for sensor to absorb thermal mass gets longer which leads to a larger gap between heating and cooling motion. In contrast, peak function at short sensor length has a narrow function profile with a sharp peak. Second, amplitude of temperature change is related to the distance between heating location and sensor location. The farther the sensors are from a heating spot, the lower the temperature change becomes. If a sensor is too far from the heat source, it is difficult to identify the time of flight due to a weak change in temperature. It is important to minimize noise at temperature change profile function so that we can comfortably calculate ToF.

As a result, we optimized our RTD sensor which has the most distinct temperature change profile at some different flowrates that we try to use in flowmeter performance test experiments. Even though we set our size and shape of RTD sensor, this sensor optimization

always need to be considered according to the experimental conditions, such as power of applied heat pulse, electrical setup and flowrate ranges.

4.2.2 Experimental setup

Water flow calibration system invented by BadgerMeter, manufacturer of products using flow measurement and control technologies, is used for high range flowrate measurement. This calibration system generates flow and controls the flow rate with mechanical pump system. Flowrates are measured with two different flowmeters in this calibration system at the same time; measurements are used as reference flowrate values. Flow rate range that this system can control is 1 to 50GPM. Considering our first flowrate target range, which is 1 to 10 GPM, the BadgerMeter calibration system is suitable to test our flowmeter.

Figure 4-1. (1) Overall water flow calibration system (2) Bypass system is connected to calibration system

The bypass system, introduced in chapter 3, makes it possible to measure higher flow rate from 1 to 30 GPM by decreasing flow speed in glass capillary due to the pressure decrease. Figure 4-2 shows overall macro-flowmeter device including bypass system. Pressure gauge is connected on the system to measure pressure drop between flow inlets of

main pipe and glass capillary. Polygon tubing is used to make liquid sample flow from main stream to the glass capillary.

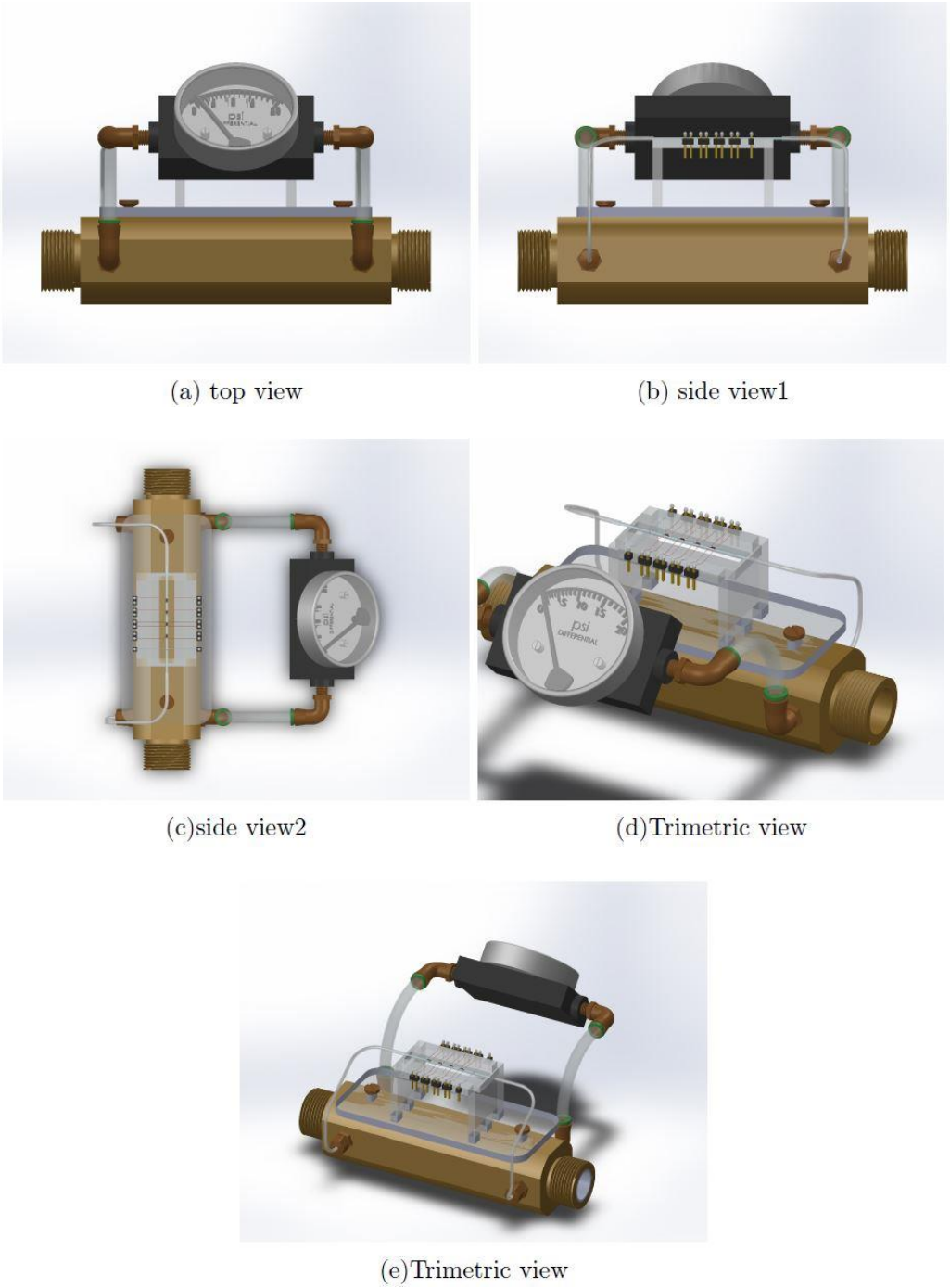

(a) top view (b) side view1

(c)side view2 (d)Trimetric view

(e)Trimetric view

Figure 4-2. Overall view of bypass system connected with flowmeter device

The size of pipe of bypass system and calibration system are intentionally made the same size so that no restriction interferes flow profile. In addition, it is easy to connect and disconnect the bypass system.

4.2.3 ToF Measurement setup

In this work, measurement setup for high flowrate range from 1 GPM to 10 GPM is introduced and illustrated in Figure 4-3.

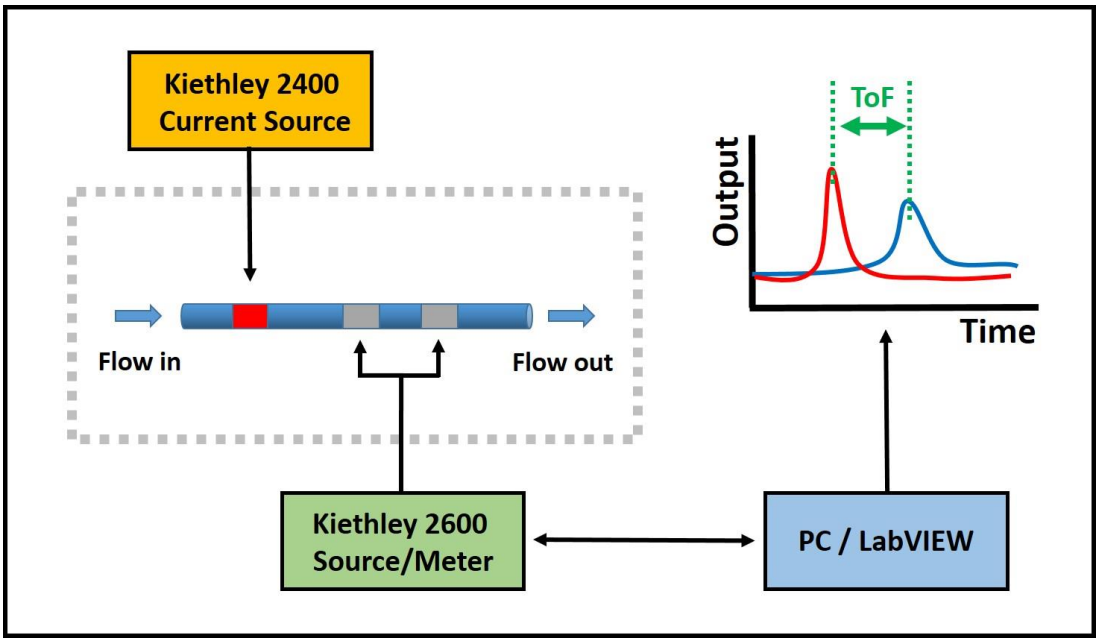

Figure 4-3. Thermal mass ToF measurement system setup configuration using Source Meter (Kiethley 2600)

In the measurement setup shown in Figure 4-3, the glass capillary is located in the middle where the fluid flows inside of the glass tube. DI (deionized) water is used as a liquid sample in this experiment. The tungsten wire (heating element) is connected to the current source (Keithley 2400) to apply heat pulses on the surface of the capillary. This current source generates DC pulse toward a heater with different pulse duration and amplitude of current. For example, a 1(A) rectangular pulse signal for 1 second generates heat from the Tungsten

wire according to the Joule heating method. The source meter (Keithley 2600) is used to measure the temperature variation at the sensor in real time. Kiethley 2600 can measure two resistance values simultaneously from the two different RTD sensors by 4 wire measurement method by giving current source (1mA). This temperature change is continuously recorded by a computer controlled by LabVIEW program until the measurement is done.

When heat is generated from the tungsten wire, the temperature of surrounding fluid inside of glass tube increases. Heated fluid is detected by the RTD sensor after some time delay depending on the fluid velocity. As the amount of current given at the RTD sensor is fixed, the resistance increases when the temperature increases due to the heated fluid coming from the heater side. Temperature change of two RTD sensors after heat pulse typically look as shown in Figure 4-4.

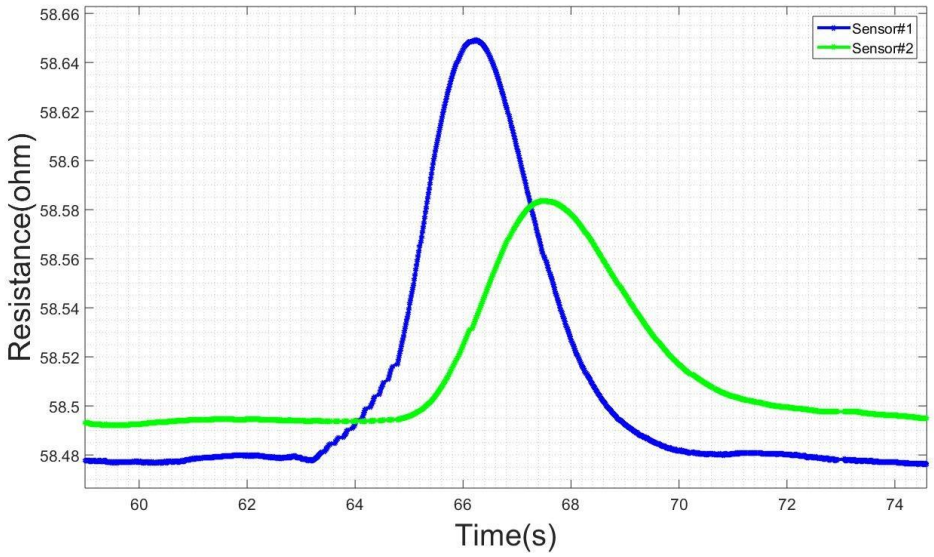

Figure 4-4. Temperature change profile after a heat pulse. Sensor1 responds faster than Sensor2 and has higher amplitude change in temperature.

Resistance variation profile recorded by LabVIEW program draws a peak shape function from both RTD sensors. The measured resistance change data values saved as ASCII code are plotted by MATLAB code. Time of flight of thermal mass is measured by

calculating the distance between a peak point of resistance change profile from one sensor and the other peak point from the other sensor. A ‘findpeaks’, Matlab built-in function code, is used to precisely measure the ToF on a scale of milliseconds.

4.2.4 Experimental result

In this experiment, thermal time of flight measurement method is used to measure the flowrate of DI water with bypass system. As we discussed in chapter 3, using bypass system, we are able to measure high flowrate range which is greater than 1 GPM. Also, we can measure different ranges of flowrate by changing the hole size of orifices. That is because fluid pressure drop from main stream to glass capillary differs due to the size of the orifice used. Therefore, it is necessary that we need to know which size of orifice should be used with bypass system to measure desired flowrate ranges.

The first experimental results show the minimum and maximum flowrate range for each different size of orifice. In this experiment, two different glass capillaries having different inner diameters, 1mm and 1.2mm, are used. Water calibration system is used to generate known flowrate in this measurement. Figure 4-5 (a) and Figure 4-5 (b) show the results of ToF using different orifices.

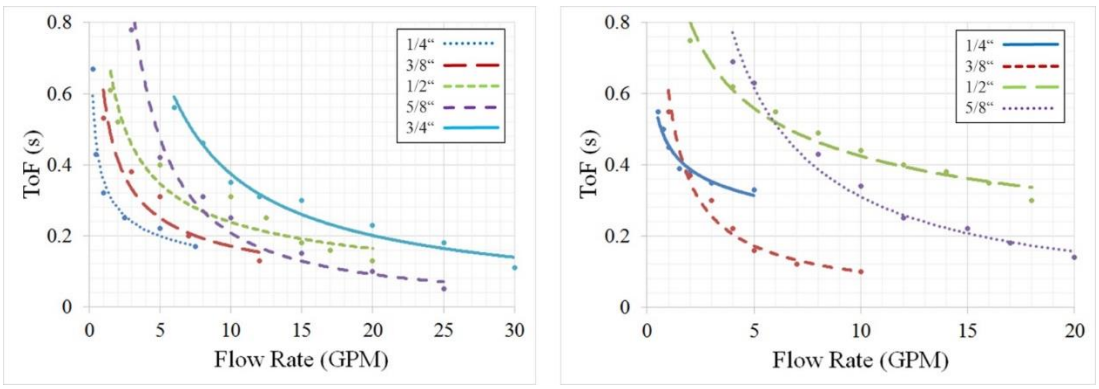

Figure 4-5. (a) ToF vs flowrate relationship at thin glass tube (inner diameter = 1mm) (b) ToF vs flowrate relationship at thin glass tube (inner diameter = 1.2mm)

As shown in the Figure 4-5 (a) and Figure 4-5 (b), the relationship between flowrate and ToF from all different orifices have inverse proportion curves as we expected. However, flowrate ranges that the flowmeter device can measure are different depending on the size of orifices and size of diameter of glass capillary. From the result, we noticed that there were distinct flowrate ranges that each orifice was able to cover. For example, while orifice that has 1/4" hole can only cover flowrate from 0.5 to 5 GPM, the one that has 5/8" hole size can measure flowrate from 5 to 20 GPM. Figure 4-6 make it easier to see the measurable ranges of flowrate of each orifice.

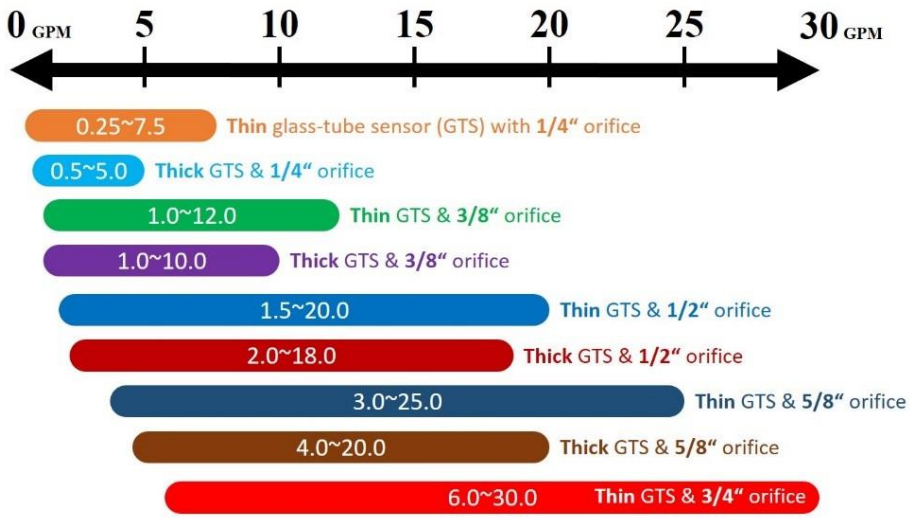

Figure 4-6. Overall measurable range of each orifice setup

In case of orifice which has 3/4" diameter hole, the measurable range of flowrate was the widest with 1mm diameter glass tube setup. As a result, we performed repeatability test and flowmeter sensitivity test with the 3/4" hole orifice.

For the repeatability test, four different flowrates were used between 1 to 10 GPM. ToF was measured 10 times for each flowrate to verify repeatability and measurement error. Table 4-2 shows the result of the experiment including applied flowrates, measured ToFs, averaged ToF, and standard deviation.

Flowrate (GPM)	1.82-1.93	2.73-2.92	4.06-4.31	5.42-5.68
ToF1(s)	0.154	0.181	0.027	0
ToF2(s)	0.073	0.138	0.103	0
ToF3(s)	0.128	0.057	0.014	0.181
ToF4(s)	0.158	0.028	0.058	0.086
ToF5(s)	0.128	0.101	0.211	0
ToF6(s)	0.112	0.102	0.201	0.062
ToF7(s)	0.143	0.1	0.029	0
ToF8(s)	0.171	0.204	0.071	0.015
ToF9(s)	0.171	0.072	0.145	0.207
ToF10(s)	0.233	0.238	0.237	0
Averaged ToF(s)	0.1471	0.1221	0.1096	0.0918
Standard deviation	0.0423	0.0673	0.0835	0.0794

Table 4-2. Measured ToFs at 4 different flowrates

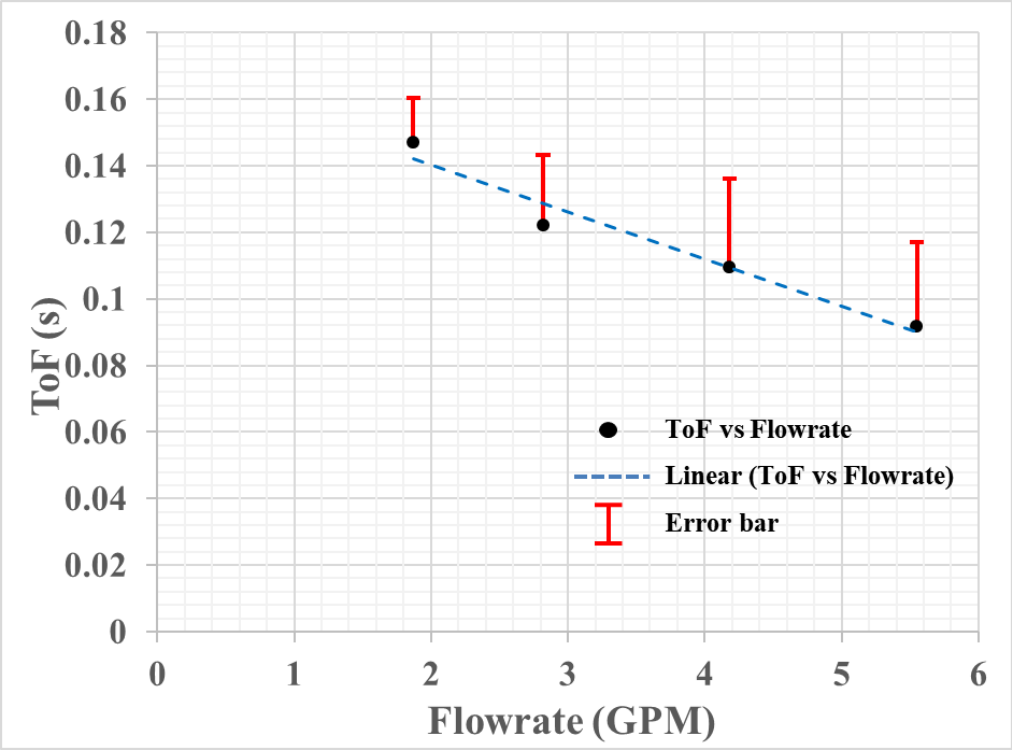

Figure 4-7. Averaged ToF vs flowrate data plot of Table 4-2 and linear fitting line

As shown in the result, Table 4-2 and Figure 4-7, values of ToF and the flowrates have inverse proportional relationship. However, overall ToF at the same flowrate has large fluctuation. From the ToF repeatability test at high flowrate, the measurement error was over 13%, which may not be suitable to use as a flowmeter when compared to available products.

4.2.5 Discussion

The flowmeter devices are fabricated and used to measure thermal mass ToF at high flowrate range using bypass system and industrial water calibration system. The advantages and disadvantages of fabricated flowmeter using bypass system are presented. This flowmeter benefits from the bypass system where the pressure drop causes lower fluid velocity that makes high flowrate measurement possible. It shows the inverse relationship between two variables, time of flight and flowrate, as we expected. Even though the relationship graph is non-linear, it is clear that ToF decreases at high flowrate.

However, ToF repeatability test using four different flowmeters shows non-negligible fluctuation according to the measurement result. ToF fluctuation occurs because of some factors. First, generated flow from water calibration system may not be stable and precise. As we can find out from the Figure 4-7, four flowrates generated by water calibration system of BadgerMeter have fluctuation by themselves during the measurement. 1.82-1.93, 2.73-2.92, 4.06-4.31, and 5.42-5.68 were unintended flowrate fluctuation from the calibration system and the failure of generating constant flowrate causes unreliable ToF results.

Second, electrical setup is not enough to measure delicate difference of ToF due to measurement speed limitations. In this electrical setup, source meter (Kiethley 2600) can measure resistance of RTD sensor 20 times per second which has time scale of millisecond. However, we are able to measure more accurate ToF between heat applied time and heat arrived time at RTD sensor when we can measure the resistance in time scale of microsecond.

In addition, ToF can be different depending on the way we analyze and calculate from the temperature change function profile. Overall, flowmeter using bypass system is not good for measuring accurate flowrate. The following section presents flowrate measurement with different electrical setup at calibration system to get rid of ToF fluctuation at same flowrate.

4.3 Flowrate measurement at low flowrate

In this section, overall information about flowrate measurement at low flowrate (less than 1ml/min) is discussed. This section includes the principle of a gravity driven flow control system and its performance. Electrical setup for this new flowrate calibration system is presented with a diagram configuration. Finally, results of thermal mass ToF flowrate measurement using this experimental setup is presented and analyzed from the point of view of the flowmeter's repeatability and sensitivity.

4.3.1 Experimental setup

A laboratory test bench was developed to try our flowmeter at low flow rate range (less than 10 ml/min). Operating principle of this flow calibration system is gravity driven flow. Liquid moves by using hydrostatic pressure, where there are no external pumping devices. Due to the fact that this system does not use external pumping force, it could be designed in cheaper, simpler, and more mobile way. Figure 4-8 shows basic principle of gravity driven flow. [35]

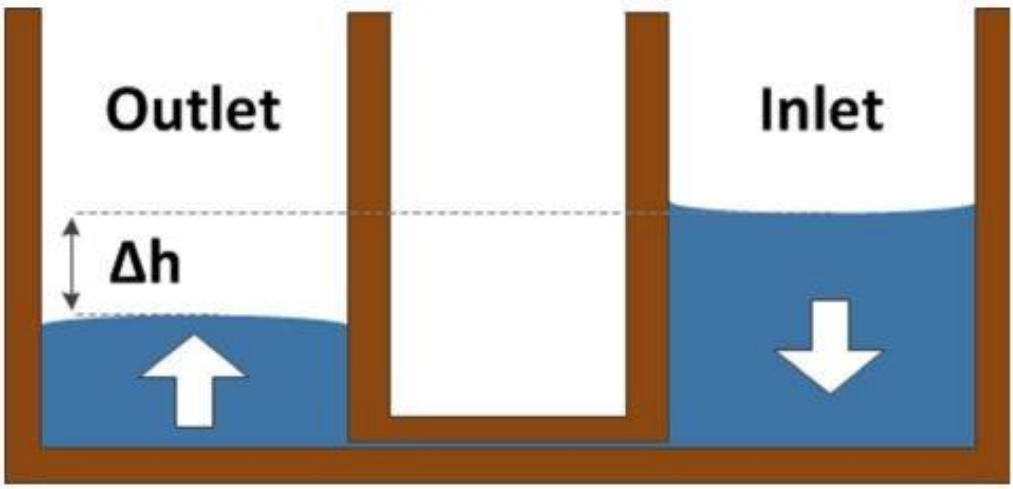

Figure 4-8. Working principle of the gravity-driven flow system. Liquid flow is driven by hydrostatic pressure created by the liquid level difference (Δh) between inlet and outlet.

In this second calibration system, the bypass system does not need to be used. Plastic tank is used to contain fluids and this tank is connected to thin glass capillary with flexible polymer tube. Fluid goes into the glass capillary where heating and sensing element are located. Then, the fluid comes out from the outlet reservoir.

By changing the height difference between inlet and outlet reservoir, fluid flowrate can be controlled. Linear translation stage with z-direction stepper motor controller helps to adjust the precise height of fluid tank. Overall working principle how fluid flows through glass capillary and measurement setup are illustrated in Figure 4-9.

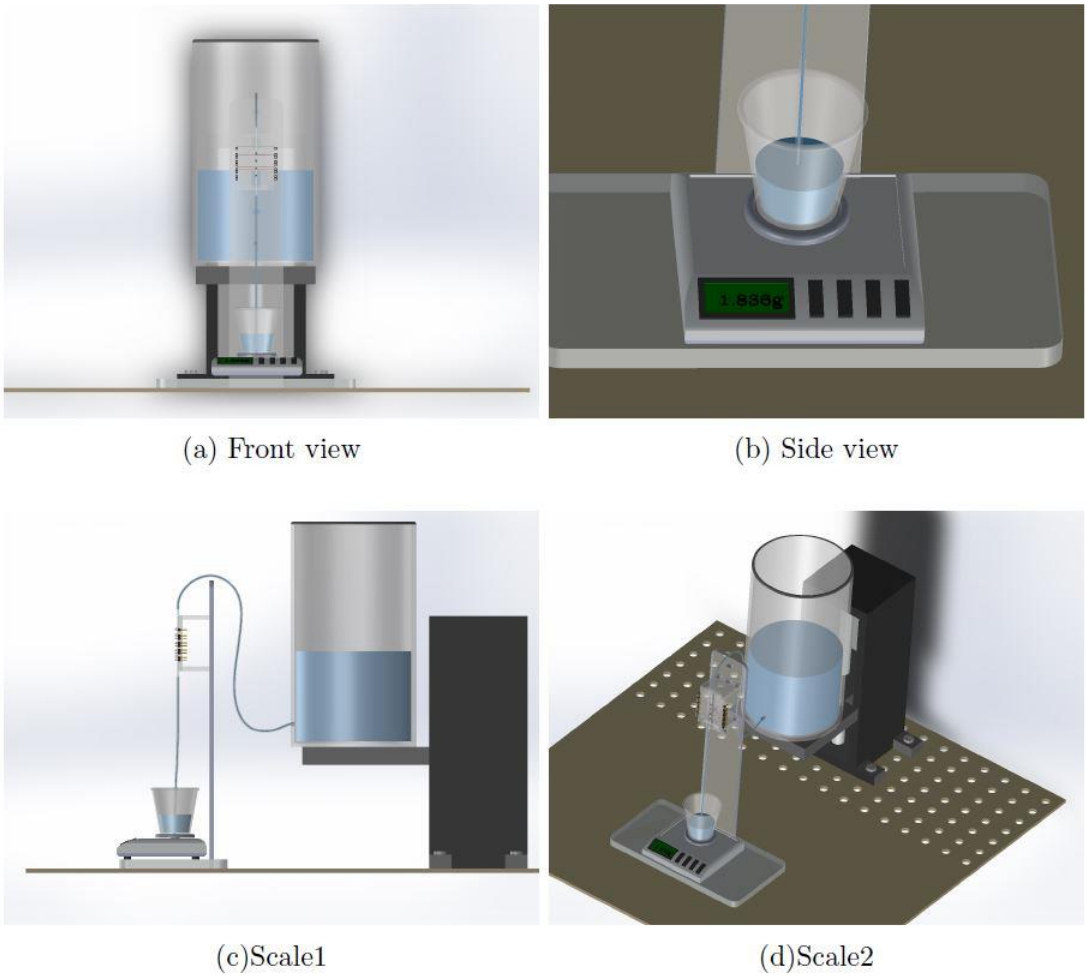

Figure 4-9. Overall configuration of gravity-driven flow calibration system

Like the BadgerMeter flow calibration system, this gravity driven flow system also needs to provide precise flowrate to use as standard flowrate value. Furthermore, the flowrate should be investigated to verify that the system functions properly in desired flowrate range.

Flowrate of this second calibration system can be measured by volumetric measurement method. Measurement of the quantity of liquid indicates flowrate. By collecting the liquid in a container from the output, we are able to calculate its flowrate with time duration between start and end time of collecting liquid. As a result, scale is integrated in this system to measure weight of liquid sample.

Measuring the weight of liquid and time duration manually results in high fluctuation at the same hydrostatic pressure and fluid condition. Scale monitoring system is invented to record weight of liquid continuously during the thermal measurement in more precise manner. There are two different ways of recording weight and they are described in the following section with its principles and data results. Gemini-20 (AWS scale) is used to measure the weight of liquid, which can weight up to 20g in 0.001g increments.

Performance test of gravity driven flow calibration system is performed as follows. First, the weight of the scale is recorded from the Liquid-crystal display (LCD) panel from programmed board (Arduino Uno). The programmed Arduino board decodes the signal from LCD panel and converts it into computer-readable data. This system can measure weight of stored liquid every 5 seconds due to the delay from signal processing. Stability test of calibration system is carried out at three different flowrate 1.1, 2.4, and 3.8 ml/min as shown in Figure 4-10. DI water is used as a liquid sample.

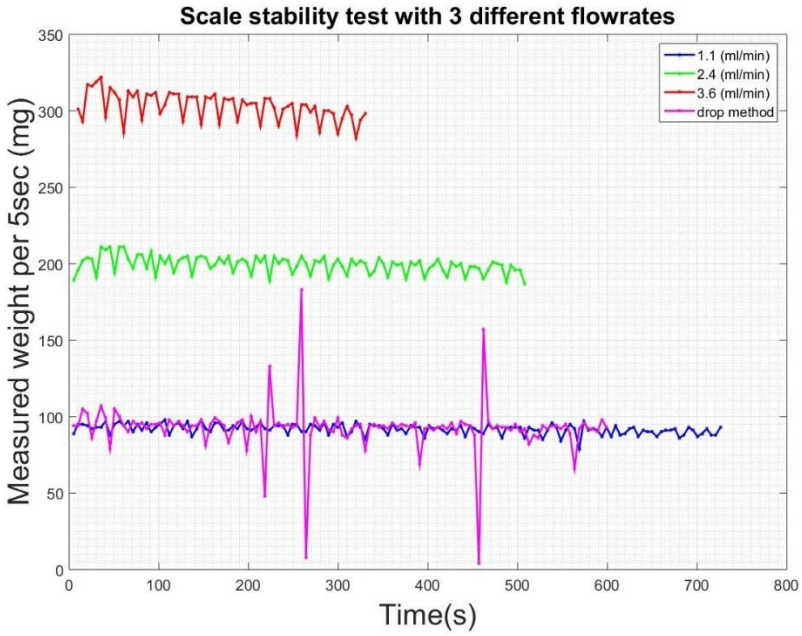

Figure 4-10. Scale stability test with LCD panel reading method at 3 different flowrates. Drained weight of water every 5 seconds is recorded.

The experimental result shows fluctuation of points which are stored water weights every 5 seconds. The fluctuation increases as the rate of flow increases. In this experiment, a tissue is attached to the tube output so that the DI water can be stored smoothly. Otherwise, potential energy of water drop from the output to the water container makes unexpected huge fluctuation in measurement which is shown as the drop method in Figure 4-10.

Second method of scale monitoring and recording is carried out by using load cell and weight sensor (HX711) with Arduino UNO. Basically, load cell is a transducer that converts force into measureable electrical output. A strain gauge, which is inside of load cell, generates an electrical signal when there is deformation. The magnitude of this electrical signal is proportional to the applied force. Weight sensor (HX711), which is analog to digital converter, amplifies the low electrical output to get accurate weight measurements. The Arduino records the amplified electrical output to the computer, as it is controlled by LabVIEW program. In contrast to the LCD reading method, this scale monitoring system can record weight 10 times per every second. Scale stability test with the second method is shown as Figure 4-11. In this experiment, 3 different flowrates, 1.55, 3.94, 6.93 ml/min, are used. [36]

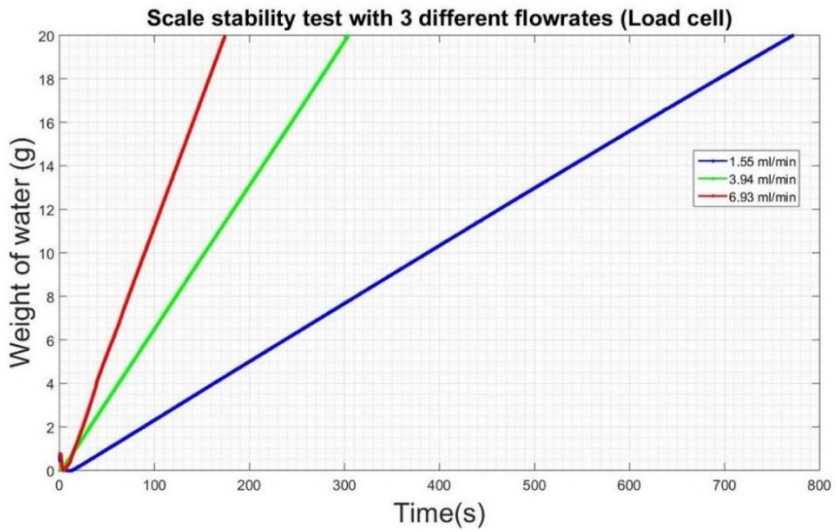

Figure 4-11. Scale stability test using load cell method at three different flowrates

Data result shows the linear relationship between time and weight of water which means that the stability of generated flowrates is high.

4.3.2 Electrical setup

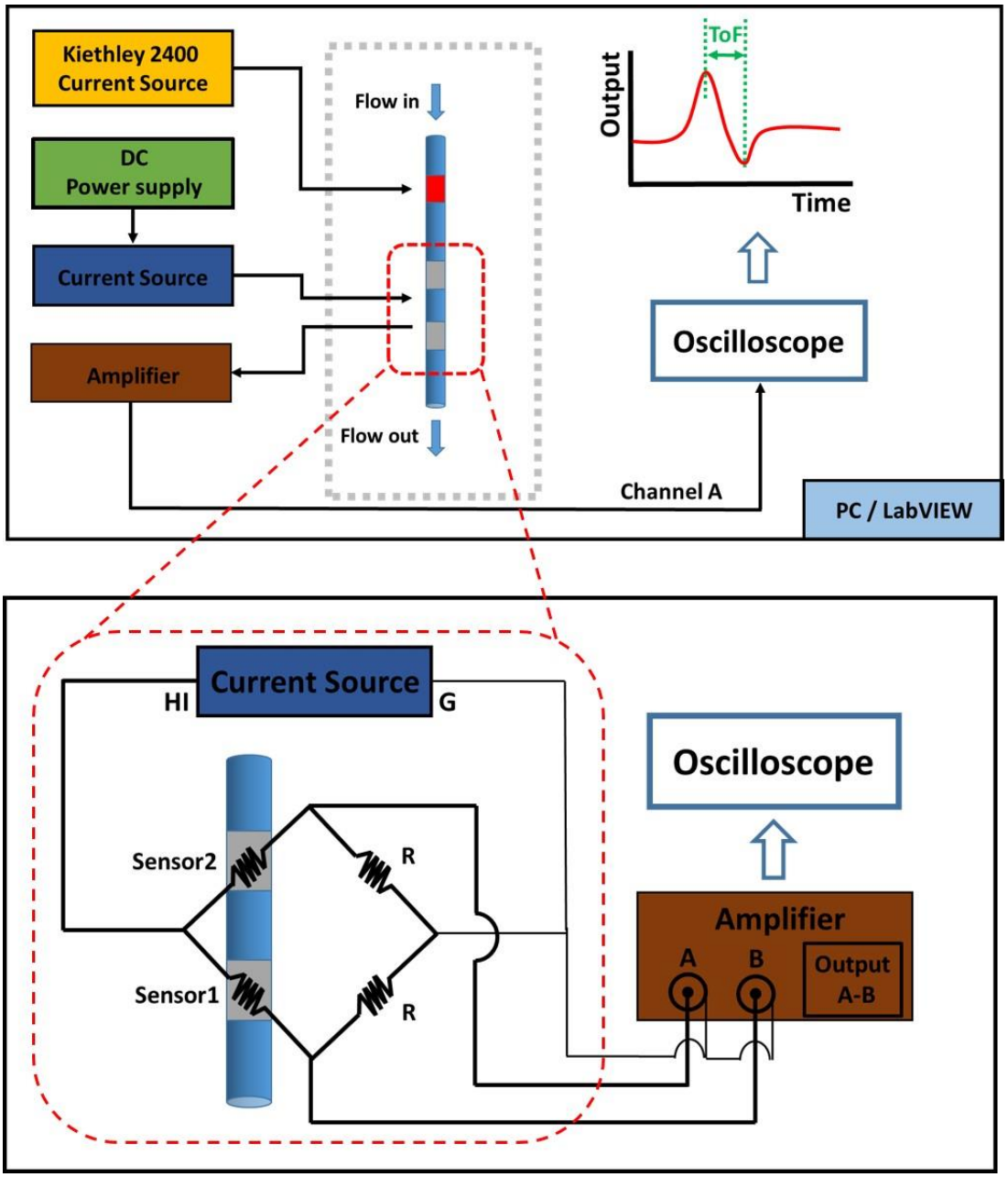

Figure 4-12. Configuration of ToF measurement setup using preamplifier and Wheatstone bridge circuit.

In this thermal mass ToF measurement, the flowmeter device which contains heating element and RTD sensors is connected to the gravity driven flow system. DI water is used as a liquid sample in this experiment as well. The tungsten wire heating method is also used in this new measurement setup to apply heat pulses to the flowing water with current source (Keithley 2400). The current source and a voltage preamplifier (Stanford SR560) are connected to the RTD sensor. The voltage preamplifier is used to amplify the signal of measured resistance change in voltage and increase the detection limit. The operation principle of the voltage preamplifier in this measurement is based on source output and gain. As shown in Figure 4-12, voltage preamplifier can measure voltage difference between two points, A and B in the diagram. From the source menu, we select function (A-B) as a desired output.

When heat is applied from the heating element, the thermal mass is developed at a portion of flowing water and temperature of the region is increased. Resistance of RTD sensors is raised by the temperature increase when the heated water passes by it. As the same amount of current is given to the RTD sensor from the current source (precision low current source), the voltage difference between two locations is measured by preamplifier and amplified by the set gain. Wheatstone bridge circuit is used as shown in Figure 4-12 for measuring accurate resistance of RTD sensors. In this measurement, 1(mA) is selected as a fixed current source. The output from the voltage preamplifier is read by an oscilloscope (Agilent DSOX 2024A). The voltage is continuously recorded during a measurement by LabVIEW program from a computer. Voltage change profile using two RTD sensors after a heat pulse is illustrated in Figure 4-13.

The most developed part of measuring ToF with this new electrical setup is in the time scale. By changing source meter, from Kiethley 2600 to oscilloscope, and sensing method, from digital to analogue, new electrical setup measures resistance of RTD sensor in microsecond time scale. Previous electrical setup for high flowrate measurement can measure

resistance 20 times per second, whereas new setup with oscilloscope can record temperature 2500 times per second.

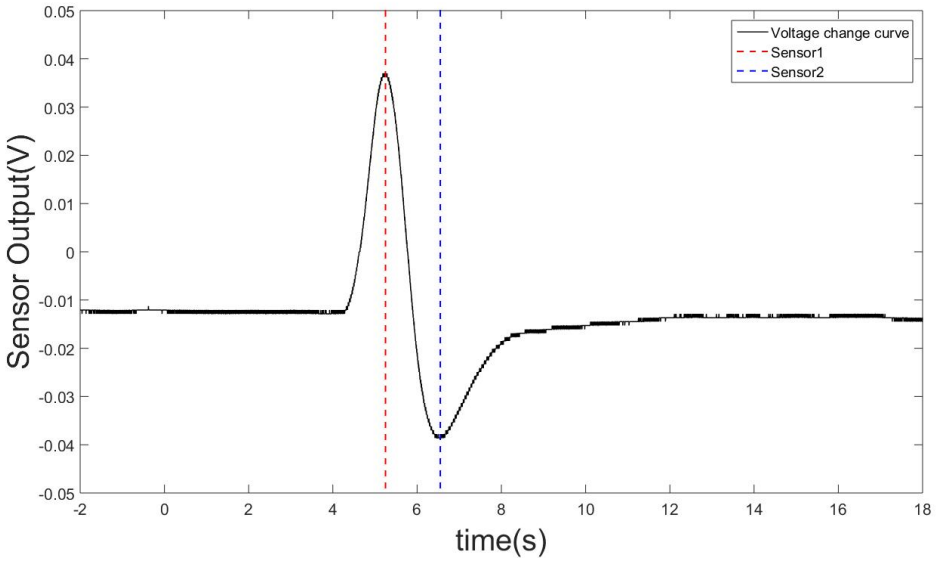

Figure 4-13. Temperature change profile from two RTD sensors using Wheatstone bridge circuit.

From Figure 4-13, the ToF of thermal mass by heat pulse is the time delay between two peaks. First peak is facing up as a result of temperature increase at sensor1. In contrast, second peak is facing down as a result of movement of heated water from sensor1 to sensor2.

ToF can be calculated differently by measuring a time delay between the time the heat pulse is applied and when heated water is detected by a RTD sensor. Figure 4-14 shows electrical setup for ToF measurement using only one sensor.

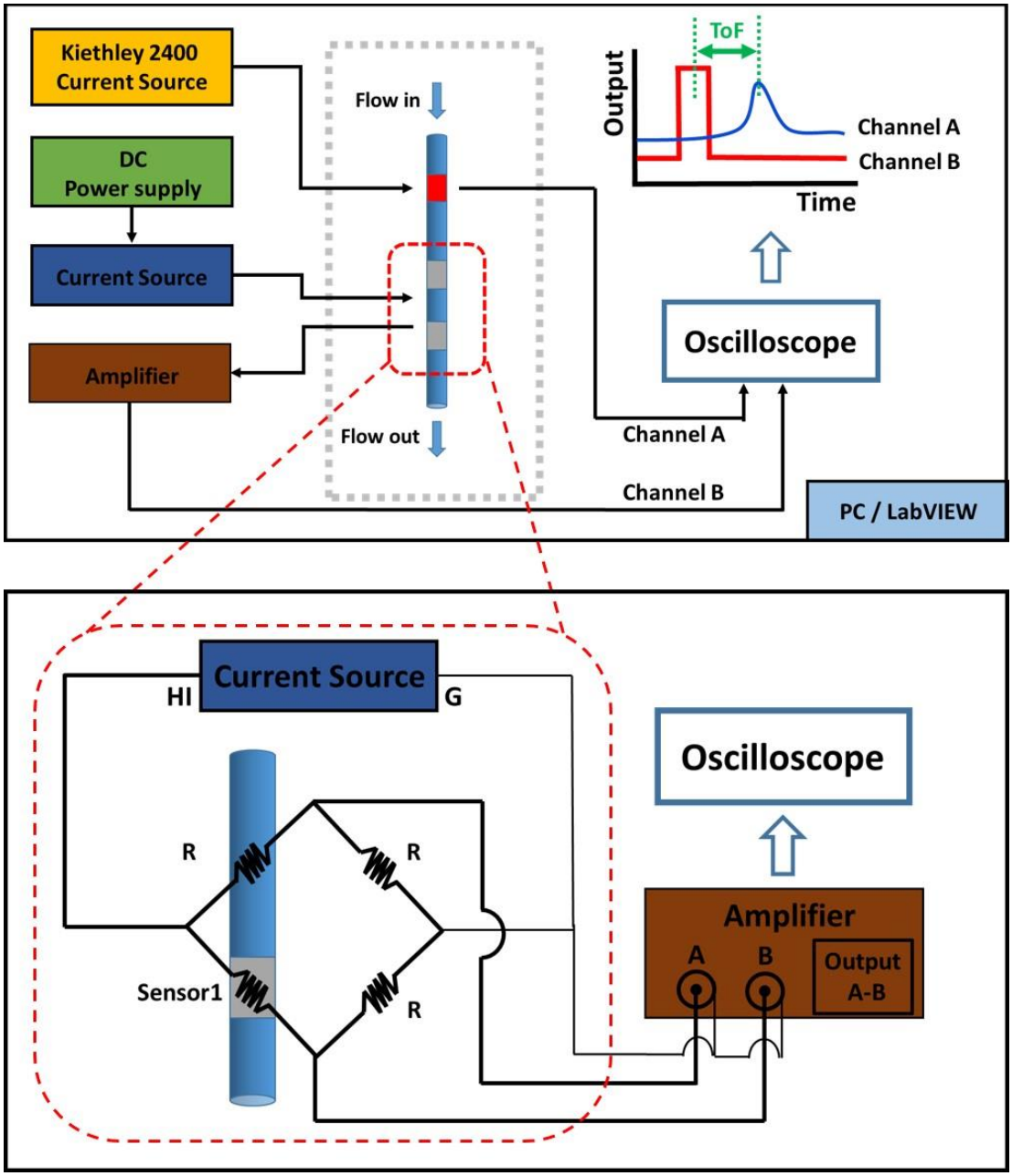

Figure 4-14. Configuration of ToF measurement setup using preamplifier and Wheatstone bridge circuit.

The Wheatstone bridge circuit is also used as shown in Figure 4-14 for measuring resistance of RTD sensor. In this experimental setup, sensor1 is the only variable resistance and the other three are reference resistors having fixed resistance value. Figure 4-15 shows the results of the temperature change function at sensor1 with heat pulse as well.

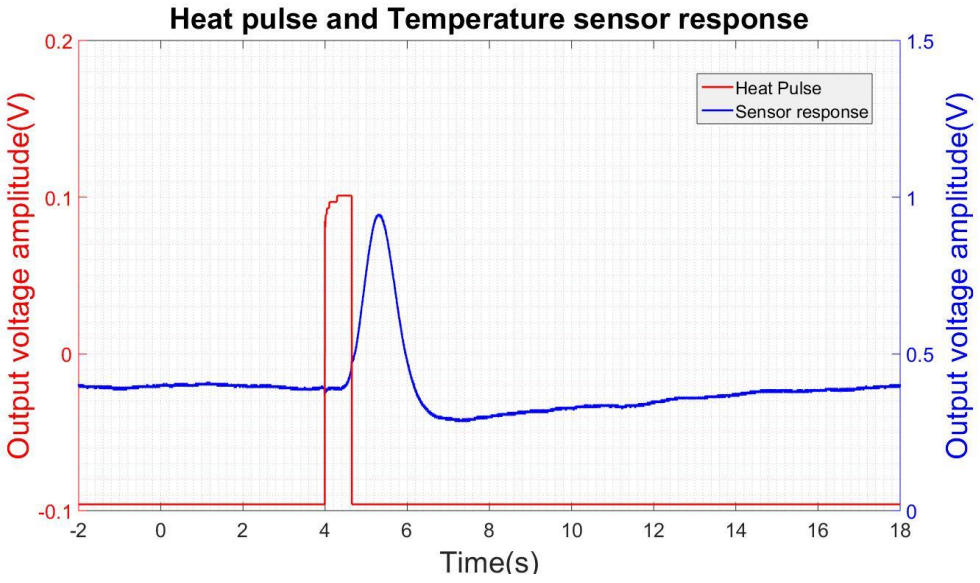

Figure 4-15. Temperature change profile from a RTD sensor using Wheatstone bridge circuit and heat pulse profile.

From Figure 4-15, ToF of thermal mass is time delay between a middle point of heat pulse and a peak point of temperature change profile from a sensor. Thermal mass ToF measurement for repeatability test was performed using both methods.

4.3.3 Experimental results

The objectives of this experiment are our flowmeter test at low flowrate range which is less than 10ml/min and the device sensitivity test at the flowrate range. Two main differences are shown in this measurement compared to the experiment setup at high flowrate measurement in the previous section. First, bypass system is not needed for measurement as velocity of fluid is not fast and measurable at low flowrate range without pressure drop. Second change is using a flowrate monitoring system to reduce calibration system error by obtaining exact flowrate at each measurement. In this experiment, one kind of glass capillary which has 1.15mm inner diameter is used to carry out the measurement.

By using gravity driven flowrate calibration system, a total of 28 different flowrates are generated which have flowrate range between 1 and 10 ml/min. ToF was measured 4

times for each flowrate to verify repeatability of flowmeter and to obtain measurement error. Table 4-3 shows measurement results including 28 different flowrates, 4 ToF data values for each flowrate, averaged ToF for each flowrate, and standard deviation.

Figure 4-16 shows ToF vs flowrate data plot. As shown in the figure, averaged ToF for each flowrate and flowrates have inverse proportional relationship. From the ToF repeatability test at low flowrate, the measurement error is 7.5%, and this error value is much less than the result of high flowrate measurement error which is 13%. Even though the targeted flowrate ranges are different between high and low flowrate measurement, the changes of experimental setup including calibration system, electrical setup, and non-use of bypass system reduce considerable amount of measurement error.

Flowrate(ml/min)	1.445	1.446	1.481	1.487	1.532	2.035	2.079	2.085	2.109	2.116	3.009	3.053	3.059	3.159
ToF (s)	1.289	1.222	1.279	1.246	1.243	0.930	0.958	0.885	0.816	0.837	0.745	0.674	0.718	0.646
ToF (s)	1.211	1.161	1.102	1.229	1.175	0.886	0.862	0.935	0.992	0.862	0.669	0.675	0.709	0.623
ToF (s)	1.307	1.342	1.199	1.195	1.230	0.814	0.948	0.862	0.939	0.910	0.733	0.693	0.745	0.707
ToF (s)	1.258	1.223	1.189	1.232	1.047	0.936	0.948	0.962	0.887	0.959	0.647	0.721	0.761	0.602
Average ToF (s)	1.266	1.237	1.192	1.226	1.174	0.892	0.929	0.911	0.909	0.892	0.699	0.691	0.733	0.644
Standard deviation	0.042	0.076	0.073	0.022	0.089	0.056	0.045	0.045	0.075	0.054	0.048	0.022	0.024	0.045
Flowrate(ml/min)	4.335	4.347	4.364	4.401	4.419	5.357	5.361	5.397	5.402	5.429	8.475	8.592	8.667	8.754
ToF (s)	0.622	0.574	0.612	0.544	0.600	0.457	0.449	0.382	0.460	0.382	0.314	0.264	0.240	0.311
ToF (s)	0.575	0.504	0.455	0.479	0.581	0.384	0.431	0.311	0.503	0.335	0.287	0.335	0.264	0.264
ToF (s)	0.601	0.551	0.597	0.445	0.503	0.447	0.358	0.455	0.407	0.358	0.288	0.239	0.216	0.265
ToF (s)	0.527	0.456	0.470	0.456	0.529	0.553	0.425	0.407	0.387	0.503	0.287	0.288	0.258	0.289
Average ToF (s)	0.581	0.521	0.534	0.484	0.553	0.460	0.416	0.389	0.439	0.395	0.294	0.281	0.244	0.282
Standard deviation	0.041	0.053	0.082	0.042	0.045	0.070	0.040	0.060	0.052	0.075	0.013	0.041	0.022	0.022

Table 4-3. Sensor optimization variables

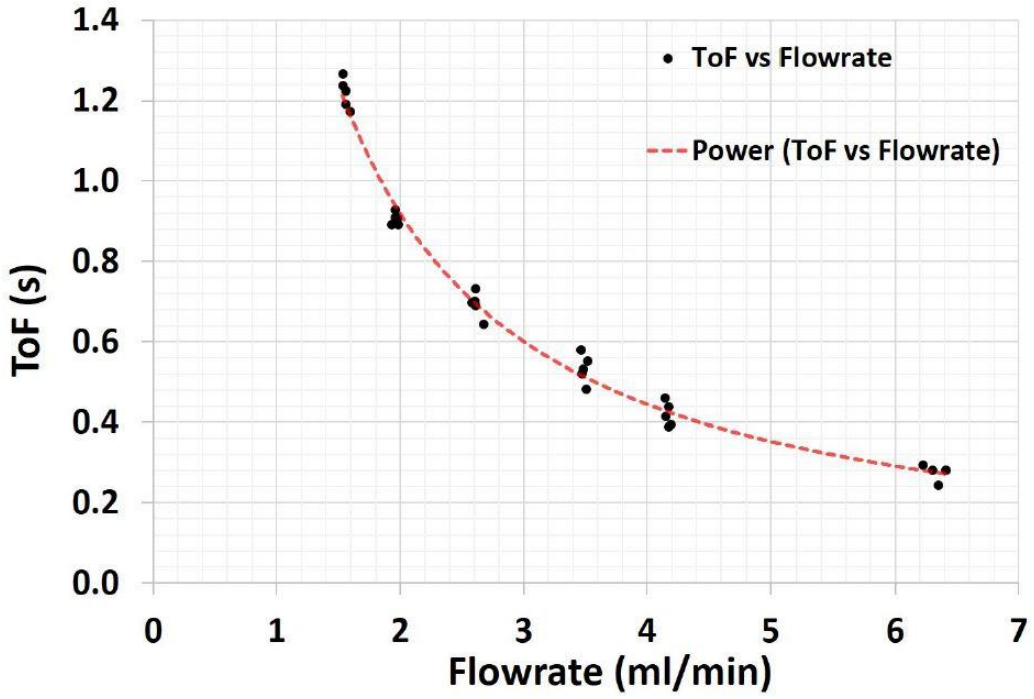

Figure 4-16. ToF vs Flowrate data plot with Table 4-16 and power series fitting curve

4.3.4 Discussion

In this section, new flowrate calibration setup and electrical measurement setup are presented to test performance of our macro-size flowmeter. Gravity driven liquid flowrate calibration system and flowrate monitoring system are developed in our laboratory and the system test show enhancement of the capability of accurate measurement.

As the ToF results show, the repeatability and measurement error at low flowrate are much more stable than the high flowrate case. In addition, the thermal mass ToF method flowmeter is promising for low-cost portable application due to an advantage of low flowrate measurement application compared to the high flowrate one that bypass component need to be used.

However, in flowmeter application, our measurement error can be one major drawback. In the device component, properties of glass capillary, stability of RTD sensor at temperature changes and response time must be considered to reduce the measurement error.

Using a glass capillary with thin wall thickness may allow our flowmeter to become a very stable device due to reduction of heat resistance from glass wall.

Overall, the presented results and analysis show the potential of the thermal measurement to apply to flowmeter applications. The results are not limited to the flowrate measurement, but the analysis of temperature change profile can be used to distinguish tested liquid samples.

Chapter 5 Conclusion and Future Works

This chapter summarizes the thesis by reviewing the thermal ToF flowmeter design, principle and device performance. Also, the design of flowrate measurement system is briefly reviewed. Ongoing research for device development is presented and future work is also discussed based on project goals and suggestions.

5.1 Conclusion

In this thesis, capabilities of thermal measurement for flowmeter using thermal mass time of flight method are investigated. The intended application of this flowmeter is characterizing the properties of flowing fluid through pipe. Among the properties, the main focus is the concept of using time of flight method to measure fluid velocity which is interpreted by temperature change. Thermal measurement uses temperature changes of flowing liquid inside of glass capillary induced by external heat flux from the surface of glass tube.

In order to increase the device sensitivity and accuracy of flowrate measurement, several approaches are selected and tested depending on flowrate ranges. This new type of flowrate measurement system has three essential parts of a flowmeter device: temperature sensor, liquid calibration system, and electrical setup for accurate measurement.

The flowmeter of this project is fabricated using micromachining processes and other sensor fabrication techniques. The metal evaporation process for thin film deposition is used to create RTD sensors in the device. Shadow mask fabrication is also performed in silicon wafer scale micromachining to make metal film with uniform thickness. Tungsten wire is used to generate a heat pulse on the flowmeter device by using Joule's heating method. Painting thermal compound between tungsten wire and glass capillary surface reduces power loss of the system and increases the transfer rate of thermal mass. Sensor parameters are

optimized to improve ToF analysis. Also, flowmeters using different thickness of glass tubes are tested and reported.

In the flowrate measurement, two water flow calibration systems are utilized differently depending on the flowrate range. For high flowrate range, a bypass system is introduced. As presented in the results, the flowmeter using bypass system shows the capability of measuring flowrate at 1-10GPM range. For low flowrate ranges, a gravity driven flow system is designed and used to enhance the sensitivity of the flowmeter as a low-power/low-cost measurement method. By introducing a flowrate monitoring system with scale sensor, more accurate flowrate measurements were possible.

Electrical setup for thermal measurement has also changed during the flowmeter development. Fast response and data recording are needed from RTD sensor to measure ToF, which is on a millisecond scale. In addition, sensor should measure small amount of temperature change for accurate liquid property measurement. Wheatstone bridge circuit temperature measurement method allows us to measure subtle change of temperature from RTD sensors.

Measuring liquid flowrate with the thermal mass ToF method shows good performance as an inferential flowmeter and has the ability to measure liquid properties. However, the measurement error needs to be reduced. The following section shows the current effort on this project to increase repeatability of the flowmeter device.

5.2 Ongoing Research and future works

The ongoing research and uncompleted work are commonly described as future work. The following list provides more theoretical and experimental work to improve the performance of our flowmeter.

First, a new design to connect the heating element and glass capillary can reduce ToF fluctuation and increase the performance of our flowmeter. Presently, tungsten wire is wound

on a glass tube and transfers heat flux through thermal conductive paste. By focusing the point where the heating wire and surface of glass tube join, the external heat flux can be transferred more uniformly and effectively. At the same time, using a glass capillary which has extremely thin wall thickness can pass the applied heat better than a thicker one.

Second, heat pulse can be created using the laser heating method. Introducing IR lasers as a heat source allows heat generation based on the absorption coefficient of a given substance. Fast and accurate heat pulse generation is the main advantage of laser heating method. In addition, heating element does not make contact with fluid pipe even on the surface.

Third, flow visualization is used to detect fluid flow development and heat transfer phenomena. As discussed in Chapter 2, fluid observation by visual inspection can bring successful analysis to the physical process. Among fluid visualization methods, interferometry imaging techniques might help to understand flow pattern inside of tube during the thermal ToF experiment. Additional measurement setup, Schlieren method, are needed to investigate fluid density change by heat pulse.

Finally, liquid type identification method using temperature measurement is being investigated. Temperature change response from a heat pulse varies with properties of the liquid samples. Each liquid sample has different density which is related to its heat transfer coefficient. More theoretical work may be needed to understand and distinguish heat diffusion property of various liquid samples.

BIBLIOGRAPHY

1. D.A. Czaplewski, R.B. Ilic, M. Zalalutdinov, W.L. Olbricht, A.T. Zehnder, H.G Craighead, A.T. Michalske, "Micromechanical Flow Sensor for Microfluidic Applications", Journal of Microelectromechanical Systems, Vol.13, No.4, pp. 576-585, Aug. 2004.

2. A. Buck, "The Importance of Mass Flow Measurement and the Relevance of Coriolis Technology," *Bronkhorst*, Mar-2017. [Online]. Available: https://www.bronkhorst.com/blog/the-importance-of-mass-flow-measurement-and-the-relevance-of-coriolis-technology-en/.

3. P. J. author. Lanasa, *Fluid flow measurement: a practical guide to accurate flow measurement*, 2nd ed. Butterworth-Heinemann, 2002.

4. Hogrefe W, "Guide to Flow Measurements*"*, Bailey-Fisher& Porter, Goettingen, Germany, 1995.

5. D. W. Spitzer, "Industrial Flow Measurement*"*, *3rd Edition*, ISA-The Instrumentation, Systems and Automation Society, 2005.

6. M. Pereira, "Flow meters: Part 1," *IEEE Instrumentation & Measurement Magazine*, vol. 12, no. 1, pp. 18–26, 2009.

7. M. Pereira, "Tutorial 20: flow meters: part 2 - Part 20 in a series of tutorials in instrumentation and measurement," *IEEE Instrumentation & Measurement Magazine*, vol. 12, no. 3, pp. 21–27, 2009.

8. M. J. Brandt, D. D. Ratnayaka, and M. Johnson, *Tworts water supply*. Oxford: Butterworth-Heinemann, 2009.

9. A. L. A. N. T. J. Hayward, *Flowmeters: a basic guide and source-book for users*. S.l.: PALGRAVE, 2013.

10. D. W. Hahn and Özısık M. Necati., *Heat conduction*. New York: Wiley, 2012.

11. Y. A. Cengel, *Heat transfer: a practical approach*. Boston: McGraw-Hill, 2003.

12. *Garbrecht, Oliver (August 23, 2017). "Large eddy simulation of three-dimensional mixed convection on a vertical plate" (PDF). RWTH Aachen University.*

13. LLC, “Convective Heat Transfer Convection Equation and Calculator,” *Engineers Edge*. [Online]. Available: https://www.engineersedge.com/heat_transfer/convection.htm. [Accessed: 20-Sep-2018].

14. “HTPage4,” *Systems Engineering*. [Online]. Available: http://www.engr.colostate.edu/~allan/heat_trans/page4/page4.html. [Accessed: 20-Sep-2018].

15. C. J. Geankoplis, *Transport Processes and Separation Process Principles (Includes Unit Operations) Fourth Edition*, 4th ed. Prentice Hall, 2003.

16. T. L. Bergman, A. Lavine, D. P. DeWitt, and F. P. Incropera, *Incroperas principles of heat and mass transfer*. Hoboken, NJ: John Wiley & Sons, Inc., 2017.

17. “December 1840: Joule's abstract on converting mechanical power into heat,” *American Physical Society*. [Online]. Available: https://www.aps.org/publications/apsnews/200912/physicshistory.cfm. [Accessed: 20-Sep-2018].

18. M. Sparks, “Theory of laser heating of solids: Metals,” *Journal of Applied Physics*, vol. 47, no. 3, pp. 837–849, 1976.

19. A. J. Smits and T. T. Lim, *Flow visualization: techniques and examples*. Singapore: World Scientific, 2012.

20. W. Merzkirch, *Flow visualization*, 2nd ed. Orlando, FL: Academic Press, 1987.

21. G. S. Settles, *Schlieren and Shadowgraph Techniques: Visualizing Phenomena in Transparent Media*. Springer, 2 ed., 2006.

22. H. G. Taylor and J. M. Waldram, “Improvements in the Schlieren method,” *Journal of Scientific Instruments*, vol. 10, no. 12, pp. 378–389, 1933.

23. H. Richard and M. Raffel, “Principle and applications of the background oriented Schlieren (BOS) method,” *Measurement Science and Technology*, vol. 6, pp. 1576–1585, 2001.

24. H. Schardin, “Schlieren methods and their applications,” *Ergeb. Exakten Naturewiss*, vol. 20, no. 303, 1942.

25. B. Atcheson, W. Heidrich, and I. Ihrke, “An evaluation of optical flow algorithms for background oriented Schlieren imaging,” *Experiments in Fluids*, vol. 46, no. 3, pp. 467–476, 2009.

26. M. Hargather and G. S. Settles, “Natural-background-oriented Schlieren imaging,” *Experiments in Fluids*, vol. 48, pp. 59–68, 2010.

27. V. Gopal, J. L. Klosowiak, R. Jaeger, T. Selimkhanov, and M. J. Z. Hartmann, “Visualizing the invisible: the construction of three low-cost Schlieren imaging systems for the undergraduate laboratory,” *European Journal of Physics*, vol. 29, no. 3, pp. 607–617, 2008.

28. S. Dalziel, G. Hughes, and B. Sutherland, “Whole-field density measurements by ‘synthetic Schlieren’,” *Experiments in Fluids*, vol. 28, no. 4, pp. 322–335, 2000.

29. B. R. Sutherland, S. B. Dalziel, G. O. Hughes, and P. Linden, “Visualisation and measurement of internal waves by synthetic Schlieren, part 1: Vertically oscillating cylinder,” *Journal of fluid mechanics*, vol. 390, pp. 93–126, 1999.

30. G. Wetzstein, R. Raskar, and W. Heidrich, “Hand-held Schlieren photography with light field probes,” in *IEEE International Conference on Computational Photography ICCP*, 2011.

31. G. S. Settles, “Colour-coding Schlieren techniques for the optical study of heat and fluid flow,” *International Journal of Heat and Fluid Flow*, vol. 6, no. 1, pp. 3–15, 1985.

32. Syed Nasimul Alam, Prabhash Kumar Panda, Animesh Kumar Singh, Heat, light and change in fine tungsten wire, Metal Powder Report, Volume 64, Issue 7, 2009, Pages 16-23, ISSN 0026-0657, https://doi.org/10.1016/S0026-0657(09)70188-2.

33. R. Paton, “Calibration and Standards in Flow Measurement,” *Handbook of Measuring System Design*, National Engineering Laboratory, Scotland, UK, 2005.

34. National measurement system., “Good practice guide: The calibration of flow meters”. https://www.tuv-sud.co.uk/uploads/images/152301105302892265O326/calibration-of-flow-meters.pdf, accessed: 20/9/2018

35. A.-J. Mäki, S. Hemmilä, J. Hirvonen, N. N. Girish, J. Kreutzer, J. Hyttinen, and P. Kallio, “Modeling and Experimental Characterization of Pressure Drop in Gravity-Driven Microfluidic Systems,” *Journal of Fluids Engineering*, vol. 137, no. 2, p. 021105, Aug. 2014.

36. PCB load & torque, “Load cell handbook : A Technical Overview and Selection Guide”. http://www.pcb.com/contentstore/MktgContent/LinkedDocuments/Load_Torque/LT-LoadCellHandbook_LowRes.pdf, 2014, accessed: 20/9/2018